ORIGINAL PAPER

Loss of TDP-43 splicing repression occurs early in the aging population and is associated with Alzheimer's disease neuropathologic changes and cognitive decline

Koping Chang[1,2] · Jonathan P. Ling[1] · Javier Redding-Ochoa[1] · Yang An[3] · Ling Li[1,4,5] · Stephanie A. Dean[4] · Thomas G. Blanchard[5] · Tatiana Pylyukh[1] · Alexander Barrett[1] · Katherine E. Irwin[1,6] · Abhay Moghekar[7] · Susan M. Resnick[3] · Philip C. Wong[1,6] · Juan C. Troncoso[1,7]

Abstract

LATE-NC, the neuropathologic changes of limbic-predominant age-related TAR DNA-binding protein 43 kDa (TDP-43) encephalopathy are frequently associated with Alzheimer's disease (AD) and cognitive impairment in older adults. The association of TDP-43 proteinopathy with AD neuropathologic changes (ADNC) and its impact on specific cognitive domains are not fully understood and whether loss of TDP-43 function occurs early in the aging brain remains unknown. Here, using a large set of autopsies from the Baltimore Longitudinal Study of Aging (BLSA) and another younger cohort, we were able to study brains from subjects 21–109 years of age. Examination of these brains show that loss of TDP-43 splicing repression, as judged by TDP-43 nuclear clearance and expression of a cryptic exon in HDGFL2, first occurs during the 6th decade, preceding by a decade the appearance of TDP-43+ neuronal cytoplasmic inclusions (NCIs). We corroborated this observation using a monoclonal antibody to demonstrate a cryptic exon-encoded neoepitope within HDGFL2 in neurons exhibiting nuclear clearance of TDP-43. TDP-43 nuclear clearance is associated with increased burden of tau pathology. Age at death, female sex, high CERAD neuritic plaque score, and high Braak neurofibrillary stage significantly increase the odds of LATE-NC. Faster rates of cognitive decline on verbal memory (California Verbal Learning Test immediate recall), visuospatial ability (Card Rotations Test), mental status (MMSE) and semantic fluency (Category Fluency Test) were associated with LATE-NC. Notably, the effects of LATE-NC on verbal memory and visuospatial ability are independent of ADNC. However, the effects of TDP-43 nuclear clearance in absence of NCI on the longitudinal trajectories and levels of cognitive measures are not significant. These results establish that loss of TDP-43 splicing repression is an early event occurring in the aging population during the development of TDP-43 proteinopathy and is associated with increased tau pathology. Furthermore, LATE-NC correlates with high levels of ADNC but also has an impact on specific memory and visuospatial functions in aging that is independent of AD.

Keywords Dementia · TDP-43 loss-of-function · Cryptic exons · Cryptic HDGFL2 · TDP-43 neuronal inclusions · LATE-NC

✉ Juan C. Troncoso
  troncoso@jhmi.edu

1 Department of Pathology, Johns Hopkins University School of Medicine, Baltimore, MD 21205, USA

2 Department and Graduate Institute of Pathology, National Taiwan University Hospital, National Taiwan University College of Medicine, Taipei 100225, Taiwan

3 Laboratory of Behavioral Neuroscience, National Institute on Aging, National Institutes of Health, Baltimore, MD 21224, USA

4 Office of the Chief Medical Examiner, State of Maryland, Baltimore, MD 21223, USA

5 Department of Pediatrics, University of Maryland School of Medicine, Baltimore, MD 21201, USA

6 Department of Neuroscience, Johns Hopkins University School of Medicine, Baltimore, MD 21205, USA

7 Department of Neurology, Johns Hopkins University School of Medicine, Baltimore, MD 21205, USA

Introduction

Dementia is a growing problem in the aging population and has become a major challenge to societies. Alzheimer's disease neuropathological change (ADNC), characterized by amyloid plaques and neurofibrillary tangles (NFT), is the most common pathology in the autopsied brains of older adults with cognitive impairment. However, ADNC is frequently accompanied by multiple neuropathologic comorbidities that contribute to cognitive impairment including transactive response DNA-binding protein of 43 kDa (TDP-43) proteinopathy [67, 77]. TDP-43 is a DNA and RNA binding protein involved in several neurodegenerative diseases, including amyotrophic lateral sclerosis (ALS), frontotemporal lobar degeneration (FTLD), and Alzheimer's disease (AD) [1, 71]. Under normal circumstances, the presence of TDP-43 is largely limited to the nucleus of neurons, but in its proteinopathic state TDP-43 is mislocalized, forming neuronal cytoplasmic inclusions (NCI) and it is excluded from the nucleus (nuclear clearance). Several studies have demonstrated that TDP-43 proteinopathy with a predominant distribution in the mesial temporal lobe is frequent in the aging population, with a prevalence ranging from 10 to 70% [3, 25, 68, 86]. In 2019, a consensus group suggested the term "Limbic-predominant Age-related TDP-43 Encephalopathy neuropathologic change" (LATE-NC), the term we will use henceforth to refer to this TDP-43 proteinopathy and associated neuropathologic changes in the aging population [69]. Increasing evidence indicates that LATE-NC is associated with cognitive decline, hippocampal atrophy, and hippocampal sclerosis [17, 31, 41–43, 45, 64, 92]. Many studies have demonstrated that LATE-NC is associated with cognitive decline independent of AD [9, 25, 29, 33, 36, 42, 45, 51, 62, 63, 65, 67, 68, 78, 79, 92]. However, we still need large-scale community-based studies with longitudinal cognitive assessments to ascertain the clinical significance of the TDP-43 proteinopathy, its relationship with ADNC and its contribution to declines in different cognitive domains either associated or independent from AD. In terms of the mechanism of TDP-43 proteinopathy, some studies have demonstrated that loss of TDP-43 splicing repression is an important mechanism in neurodegenerative diseases including ALS and FTLD [50, 83]. However, the age of onset of TDP-43 loss-of-function in the human brain and its relationship with nuclear clearance and TDP-43 NCI remain unknown. Here, we use clinical and neuropathologic data from participants in the Baltimore Longitudinal Study of Aging (BLSA), a community-based cohort study, to explore LATE-NC and TDP-43 splicing repression in the aging population. All participants were cognitively normal at enrollment and had periodic longitudinal cognitive assessments. We also assessed for TDP-43 splicing repression in a younger forensic autopsy cohort. To examine the cryptic exon inclusion in cases with LATE-NC, we used RNA in situ hybridization (BaseScope) followed by immunofluorescent demonstration of a cryptic exon-encoded neoepitope within HDGFL2 using a recently characterized monoclonal antibody [35]. Our results showed that high levels of ADNC significantly increase the odds of LATE-NC, which is associated with accelerated decline in multiple cognitive domains. Notably, there are associations of LATE-NC with verbal memory and visuospatial ability that are independent of ADNC. Importantly, our data revealed that loss of TDP-43 splicing repression first occurs in the aging population during the 6th decade of life and a decade preceding the appearance of TDP-43 + NCIs.

Materials and methods

Subjects

Participants in this study were 309 individuals from the BLSA autopsy cohort (age range 57–109, mean age 88.5 years). The BLSA is a prospective study of community-dwelling volunteer participants begun in 1958 and conducted by the National Institute on Aging. Participants had normal cognition at the time of BLSA enrollment. Neuropsychological assessments, neurological, laboratory and clinical evaluations were conducted during each visit. The BLSA visit schedule has changed over time. Participants were typically seen every two years before 2003. Since then, participants were seen every 4 years for age < 60 years, every 2 years for 60–79 years, and annually for ≥ 80 years until they are untestable or expire [90]. The BLSA study was approved by the local Institutional Review Board and the National Institute on Aging. Written informed consent was obtained at each visit from all participants. An additional 24 donated autopsy brains from individuals 21–68 years of age (mean age 43 years) were included for examination of TDP-43 nuclear clearance in a younger age group. Individuals in this younger autopsy cohort did not have history of cognitive decline, but no cognitive evaluation was available. These autopsies were performed at the Office of The Chief Medical Examiner (OCME) of the State of Maryland in Baltimore and accessioned by the University of Maryland Brain and Tissue Bank with appropriate consent from the next-of-kin. Research proceedings were approved by institutional review boards. All brains were examined in the Division of Neuropathology at Johns Hopkins Medicine under a protocol approved by the JHU IRB.

BLSA cohort cognitive assessments

Subjects enrolled in the BLSA cohort had comprehensive longitudinal cognitive assessments. The Combined Clinical Dementia Rating (CDR) scale [61] was administered at 1- to 2-year intervals to all autopsy study participants [90]. Clinical and neuropsychological data from participants were reviewed at consensus conferences if their Combined Clinical Dementia Rating scale score was ≥ 0.5 or if they had > 3 errors on the Blessed Information-Memory-Concentration Test [27]. After death, subjects were adjudicated as having normal cognition, mild cognitive impairment (MCI), or dementia at a consensus diagnostic meeting by study examiners who were unaware of the neuropathologic diagnoses. Diagnoses of dementia and AD, respectively, were based on criteria outlined in the Diagnostic and Statistical Manual of Mental Disorders, third edition, revised [2], and the National Institute of Neurological and Communication Disorders and Stroke–Alzheimer's Disease and Related Disorders [56]. MCI was based on the Petersen criteria [74].

For the analysis of longitudinal cognitive trajectories, we included all longitudinal cognitive assessments conducted within 20 years prior to participants' death, from individuals who were ≥ 60 years old at the time of data collection, and whose assessments were conducted in or after 1993. The final analytic sample of cognitive function included 243 participants with 1405 cognitive assessments. The cognitive assessments include Mini Mental State Exam (MMSE) [26], California Verbal Learning Test (CVLT) immediate recall across five learning trials to assess verbal memory [18], Trail Making Tests A and B to measure attention, psychomotor speed and executive function [76], Card Rotations test to measure visuospatial ability [22, 91], Letter and Category Fluency tests to measure phonemic and semantic fluency, respectively [7, 72]. A detailed description of the cognitive measures and procedures have been published previously [54].

Neuropathological assessments

This study included 309 autopsy brains from BLSA participants and 24 brains from the younger autopsy cohort. After autopsy, all brains from the BLSA cohort were fixed in neutral buffered formalin for 2 weeks. Following external examination, brains were cut in coronal slabs and diagnostic tissue blocks were dissected from the left cerebral hemisphere in most instances. For microscopic examination, tissues from the middle frontal gyrus, superior and middle temporal gyri, inferior parietal cortex, precuneus, occipital cortex, cingulate gyrus, basal ganglion, thalamus, amygdala, hippocampus, midbrain, pons, medulla, and cerebellum were obtained. Brains from the younger autopsy cohort were examined and cut fresh in coronal slabs after autopsy. Tissues from the middle frontal gyrus, motor cortex, superior and middle temporal gyri, inferior parietal cortex, occipital cortex, basal ganglion, amygdala, hippocampus, midbrain, pons, medulla, and cerebellum were obtained. Tissues were fixed in 10% neutral buffered formalin, dehydrated in graded alcohols, cleared in xylene, and embedded in paraffin. Tissue sections were cut at 10 μm and stained with H&E. For BLSA brains, Hirano-silver stain was performed on middle frontal gyrus, superior and middle temporal gyri, inferior parietal cortex, precuneus, occipital cortex, amygdala, and hippocampus. Immunohistochemistry (IHC) of β-amyloid was performed on thalamus, midbrain, and cerebellum. IHC of phosphorylated tau was performed on middle frontal gyrus, superior and middle temporal gyri, inferior parietal cortex, occipital cortex, thalamus, amygdala, hippocampus, midbrain, and pons. IHC of α–synuclein was performed on cingulate gyrus, amygdala, and midbrain. Additional IHC was performed in brains with suspected histological abnormalities. For young autopsy cohort brains, IHC of phosphorylated tau was performed on middle frontal gyrus, amygdala, entorhinal cortex, and pons. IHC of β-amyloid was performed on middle frontal gyrus and amygdala. Additional IHCs including phosphorylated tau and β-amyloid were performed in brains with positive phosphorylated tau and β-amyloid staining or suspected histological abnormalities. IHC of α–synuclein was performed in brains with suspected Lewy body.

IHC of TDP-43 was performed using both phosphorylation-independent and phosphorylation dependent TDP-43 antibodies. The phosphorylation-independent antibody recognizes all forms of TDP-43 protein. The phosphorylation dependent TDP-43 antibody recognizes TDP-43 phosphorylation at Serine 409/410 and was used to evaluate TDP-43+ NCIs as well as other staining patterns. Phosphorylation independent TDP-43 antibody was used to assess the nuclear localization of TDP-43 and also TDP-43+ NCIs. In all brains, tissue sections of the amygdala and hippocampus were immunostained with both types of anti-TDP-43 antibodies. Sections of middle frontal gyrus were stained in cases with any positive staining in the amygdala, hippocampus, entorhinal cortex, or adjacent structures. Sections of precuneus and inferior parietal lobule were stained in randomly selected cases encompassing all LATE-NC stages (n = 22), including 7 cases of stage 0, 2 cases of stage 1, 10 cases of stage 2, and 3 cases of stage 3.

To examine the relationship of LATE-NC and tau pathology, we examined tau pathology in the dentate gyrus. Tau-positive granule cells were counted manually by a neuropathologist blinded to the pathologic diagnosis and TDP-43 status. The counts of tau-positive granule cells were adjusted by the lengths of the dentate gyrus granule cell layers.

Immunohistochemical (IHC) method

IHC stains were conducted on 10-μm or 40-μm thick sections from formalin fixed paraffin embedded tissues. Each section was deparaffinized with xylene and rehydrated through graded alcohols and water followed by heat-based antigen retrieval. Pretreatment with 88% formic acid for 5 min was performed for α-synuclein and β-amyloid immunostaining. Endogenous peroxidases were blocked using a 3% hydrogen peroxide solution. The slides were blocked with 3% normal goat serum in Tris-buffered saline (TBS) solution for 1 h at room temperature (RT). Primary antibodies (anti-β-Amyloid, 1:500, clone 6E10, mouse, 803023, BioLegend, San Diego, CA; anti- phosphorylated tau, 1:200, clone AT8, MN1020, Invitrogen, Waltham, MA; anti-α–synuclein, 1:500, mouse, clone 42, 610787, BD, Franklin Lakes, NJ; anti-TDP-43 (phosphorylation independent), 1:1000, rabbit polyclonal, 12782-1-AP, Proteintech, Rosemont, IL; anti-TDP-43 phosphorylation at Serine 409/410, 1:200, rat, clone 1D3, 829901, BioLegend, San Diego, CA) were applied for 1 h at RT. Slides were washed with TBS. The biotinylated horseradish peroxidase secondary antibodies (Abcam) were applied for 1-h at RT. After washing with TBS, ABC (Vector Laboratories) and DAB kits (Vector Laboratories) were used. After washing, slides were counterstained with hematoxylin, dehydrated by alcohol and xylene, and coverslipped using Permount mounting medium (Fisher Chemical).

Assessment of Alzheimer's and other neurodegenerations

For assessment of neurodegeneration, we used Hirano-silver stained sections to score the density of the NP according to CERAD criteria [59] and stage NFT according to Braak [10]. β-amyloid distribution was assessed using anti-β-Amyloid antibody according to the Thal phase system [84]. Alzheimer's disease neuropathologic change was staged according to NIA-AA criteria [34]. Lewy body pathology was examined using the anti-α–synuclein antibody and scored according to Third Report of the Dementia with Lewy Bodies Consortium [55]. The diagnosis of primary aging-related tauopathy (PART) was formulated according to Crary et al. [15].

Immunofluorescent (IF) staining method for evaluation of TDP-43 nuclear clearance

TDP-43 nuclear clearance was evaluated in granule cells of the hippocampus dentate gyrus using IF staining with the phosphorylation independent anti-TDP-43 antibody. We counted only cells with granule cell morphology. IF staining was performed by triple labeling with phosphorylation independent TDP-43 (1:200), phosphorylation dependent TDP-43 (1:200), and NeuN (1:1000, mouse, clone A60, MAB377, MilliporeSigma, Burlington, MA) antibodies on 10-μm thick sections from formalin fixed paraffin embedded tissue blocks. Each section was deparaffinized with xylene and rehydrated with graded alcohols, and water. For antigen retrieval, tissue sections were microwaved for 10 min in citrate buffer (ab93678, Abcam). All sections were blocked with 3% normal goat serum in Tris-buffered saline (TBS) solution with 0.2% Triton X-100 for 1 h at RT. The primary antibodies were applied and incubated overnight at 4 °C. After washing with TBS, the secondary antibodies were applied for 1 h at RT: Alexa Fluor 488 anti-Rabbit IgG (1:400, ab150077, Abcam), Alexa Fluor 568 anti-Mouse IgG (1:400, ab175701, Abcam), Alexa Fluor 647 anti-Rat IgG (1:400, ab150159, Abcam), and DNA stain with DAPI (1:1000, Cat#10236276001, Roche). After washing with TBS, sections were coverslipped using ProLong Gold Antifade Mountant (P36930, Invitrogen). Slides were examined on a Leica Mica confocal microscope.

Cryptic exon-encoded neoepitope: IF staining

For IF staining of a TDP-43 dependent cryptic peptide, a mouse monoclonal antibody recognizing the cryptic exon-encoded neoepitope in Hepatoma-Derived Growth Factor-Like protein 2 (HDGFL2) was used [35] (Supplementary Information). Cryptic HDGFL2 was co-labeled with phosphorylation independent TDP-43 (1:200) and phosphorylation dependent TDP-43 (1:200). Antigen retrieval using HistoVT One (Nacalai Tesque, Kyoto, Japan) 95 °C 30 min was performed. IF staining method is as described above.

A peptide competition test was performed to evaluate the specificity of the cryptic HDGFL2 antibody IF staining. Three different peptides with overlapping amino acid sequences from the cryptic HDGFL2 sequence were tested: peptide 1: EPTIWFGKGHSGMLASEGREA; peptide 2: SEGREAVLTRLHESERVRKQ; peptide 3: HESERVRKQERERDTEERRE. Five times peptide to antibody by weight were added in the primary antibody mixture containing cryptic HDGFL2 antibody, phosphorylation independent TDP-43 antibody, and phosphorylation dependent TDP-43 antibody. IF staining was performed as described above. Slides were examined on a Leica Mica confocal microscope.

TDP-43 dependent cryptic exon: RNA in situ hybridization

For examination of cryptic exon containing RNA transcripts, BaseScope™ probes (Advanced Cell Diagnostics, Newark, CA) were designed for TDP-43 dependent cryptic exon containing transcripts of *HDGFL2*. Assays were conducted using a BaseScope™ RED Reagent Kit according to the

manufacturer's protocol in 5 brains with TDP-43+ NCIs, 5 brains with TDP-43 nuclear clearance only, and 5 brains without TDP-43 pathology. Sections were deparaffinized, rehydrated, and blocked for endogenous peroxidases with H2O2, pre-treated with ACD RNAScope Target Retrieval Reagents. The slides were incubated in Protease IV solution for 30 min at 40 °C, and then in probe solution for 2 h at 40 °C in the HybEZ II Oven. Amp reagents 1–8 were used according to the protocol. Slides were incubated in Fast Red for 10 min, counterstained with hematoxylin, dried, and coverslipped with VectaMount. Number of cryptic *HDGFL2* transcripts (red dots) in 1000 granule cells in the dentate gyrus per brain were counted for quantification of cryptic *HDGFL2* transcripts.

Statistical methods

Demographic, clinical, and neuropathologic characteristics were compared between the LATE-NC positive and negative groups using t-test and Chi-square ($\chi 2$) test, depending on the assessed variable. The number of cryptic *HDGFL2* transcripts between pairs of different groups were compared using the Mann–Whitney test. For assessment of tau pathology in the dentate gyrus in different groups, the Kruskal–Wallis test was used for comparing all three groups and the Mann–Whitney test was used for comparing pairs.

To investigate the effects of age, sex and APOE ε4 status on the probability of LATE-NC presence, we used logistic regression analysis with LATE-NC as the outcome. The initial full model included the predictors of sex, APOE ε4 (carrier vs. non-carrier), age at death, and all 2-way interactions among these three factors. Backwards elimination was used to reduce the model for all the interactions at the $p = 0.1$ level.

We used separate logistic regression to model the relationship between CERAD scores and Braak stages and probability of LATE-NC presence. CERAD scores and Braak stages were used separately as continuous predictors, assuming linearity between logit of LATE-NC presence with CERAD scores and Braak stages. Models were conducted without and with adjustments of age of death, sex and APOE.

We used separate linear mixed effects models with each longitudinal cognitive measure as the outcome to estimate the effect of LATE-NC on the longitudinal cognitive trajectories. Time to death (years) was used as the time variable in linear mixed effects models. Two sets of models were tested for each cognitive measure. The first sets of models included covariates of sex and age of death. The fixed effects included LATE-NC (presence vs absence), age at death, sex, time, time square, and the interactions of LATE-NC, age at death and sex with time and time square. Since the cognitive trajectories were modeled to be quadratic and nonlinear, the effects of LATE-NC on cognitive trajectories were tested using F test with 2 degrees of freedom so that interactions of LATE-NC with time and time square were tested simultaneously. If the effect of LATE-NC on prior cognitive trajectories was significant, we estimated the cognitive performance difference between LATE-NC groups at 1 year, 5 years and 10 years prior to death based on the model for illustration purposes. For the second set of models, we additionally included CERAD scores and Braak stages as covariates. Random effects of the model included intercept, time and time square with unstructured covariance. The statistical tests were two-sided with a type I error of 0.05 unless stated otherwise.

All the analyses were conducted in SAS 9.4 (Cary, NC).

Results

Characteristics of participants in the BLSA cohort

This study included 309 deceased BLSA participants. Males outnumber females because the BLSA cohort was initially limited to men with enrollment of women beginning in 1978. Mean age at death was 88.5 years (ages range 57–109 years). The participants were predominantly white (93.5%), 33.0% had normal cognition, 14.6% had MCI, and 52.4% had dementia before death. Other demographic and clinico-pathological characteristics including CERAD neuritic plaque (NP) score and Braak neurofibrillary tangle (NFT) stage for ADNC are summarized in Table 1.

Clinical and pathological features of TDP-43 proteinopathy

Among the 309 BLSA participants, 118 (38.2%) had LATE-NC comprised of TDP-43+ neuronal cytoplasmic inclusions (NCIs) accompanied by nuclear clearance of TDP-43 (Fig. 1a–c). According to the recently updated LATE-NC staging system [70], among the 309 BLSA participants, 27 (8.74%) are stage 1a, 9 (2.91%) are stage 1b, 71 (23.0%) are stage 2, and 11 (3.56%) are stage 3. Other LATE-NC, including dense networks of TDP-43+ neurites (Fig. 1d), TDP-43+ glial staining (Fig. 1e–g), subpial and subependymal TDP-43+ processes (Fig. 1h–j), and perivascular TDP-43+ pattern (Lin bodies) (Fig. 1k, l) [49] were also observed. TDP-43+ glial staining or subpial and subependymal TDP-43+ cell processes in the absence of NCIs were present in 12 (3.88%) brains, corresponding to LATE-NC stage 1c, which is not included in the LATE-NC positive group in all the following analyses [70] (Table 1). Perivascular TDP-43 pathology is mostly found in brains with TDP-43+ NCIs. From a total of 118 brains with TDP-43+ NCIs, 62 (52.5%) had perivascular TDP-43 pathology, while of 44

Table 1 Demographics and clinicopathologic characteristics of the BLSA autopsy participants (n = 309)

Characteristics	Total	LATE-NC positive	LATE-NC negative	p value
Case number (%)	309	118 (38.2%)	191 (61.8%)	
Age at death				
Mean (SD)	88.5 (8.4)	91.3 (6.7)	86.8 (8.8)	**< 0.001**
Range	57.6 – 109.5	68.9 – 107.1	57.6 – 109.5	
Sex				< 0.001
Male	190 (61.5%)	56 (47.5%)	134 (70.2%)	
Female	119 (38.5%)	62 (52.5%)	57 (29.8%)	
Race				0.616
White	289 (93.5%)	114 (96.6%)	175 (91.6%)	
African–American	14 (4.5%)	4 (3.67%)	10 (5.23%)	
Other	6 (2.0%)	0 (0%)	6 (3.14%)	
CERAD NP score [59]				**< 0.001**
0	87 (28.5%)	15 (12.8%)	72 (38.3%)	
A	38 (12.5%)	15 (12.8%)	23 (12.2%)	
B	122 (40%)	57 (48.7%)	65 (34.6%)	
C	58 (19.0%)	30 (25.6%)	28 (14.9%)	
Braak NFT stage [10]				**< 0.001**
0	4 (1.3%)	0 (0%)	4 (2.1%)	
I	12 (4.0%)	1 (0.85%)	11 (5.88%)	
II	60 (19.7%)	11 (9.32%)	49 (26.2%)	
III	55 (18.1%)	15 (12.7%)	40 (21.4%)	
IV	114 (37.5%)	54 (45.8%)	60 (32.1%)	
V	24 (7.9%)	11 (9.32%)	13 (69.5%)	
VI	35 (11.5%)	25 (21.2%)	10 (5.34%)	
APOE ε4 carrier				0.126
ε4 carrier	75 (26.1%)	34 (31.8%)	41 (22.8%)	
Non-ε4 carrier	212 (73.8%)	73 (68.2%)	139 (77.2%)	
Cognitive function				**< 0.001**
Normal	102 (33.0%)	15 (12.7%)	87 (45.5%)	
MCI	45 (14.6%)	13 (11.0%)	32 (16.8%)	
Dementia	162 (52.4%)	90 (76.3%)	72 (37.7%)	
Neuropathologic diagnosis				**< 0.001**
ADNC	144 (46.6%)	65 (55.1%)	79 (41.4%)	
ADNC + LBD	18 (5.83%)	8 (6.78%)	10 (5.24%)	
ADNC + vascular dementia	36 (11.7%)	19 (16.1%)	17 (8.90%)	
ADNC + LBD + vascular dementia	5 (1.62%)	3 (2.54%)	2 (1.05%)	
ADNC + other pathology	9 (2.91%)	5 (4.24%)	4 (2.10%)	
LBD	4 (1.29%)	2 (1.69%)	2 (1.05%)	
LBD + vascular dementia	2 (0.65%)	1 (0.85%)	1 (0.52%)	
Vascular dementia	15 (4.85%)	2 (1.69%)	13 (6.80%)	
PART	63 (20.4%)	9 (7.63%)	54 (28.3%)	
Other pathology	11 (3.56%)	4 (3.39%)	7 (3.66%)	
Normal	2 (0.65%)	0 (0%)	2 (1.05%)	
TDP-43 pathology				
NCIs	118 (38.2%)			
glia	71 (23.0%)			
subpial/subependymal	31 (10.0%)			
perivascular	64 (20.7%)			
LATE-NC stage [70]				
Stage 0	179 (57.9%)			
Stage 1	48 (15.5%)			

Table 1 (continued)

Characteristics	Total	LATE-NC positive	LATE-NC negative	*p* value
Stage 1a	27 (8.74%)			
Stage 1b	9 (2.91%)			
Stage 1c	12 (3.88%)			
Stage 2	71 (23.0%)			
Stage 3	11 (3.56%)			

Significant *p* values are bolded

ADNC Alzheimer's disease neuropathologic change, *LATE-NC* limbic-predominant age-related TDP-43 encephalopathy neuropathologic change, *LBD* Lewy body disease, *NFT* neurofibrillary tangles, *NP* neuritic plaques, *PART* primary age-related tauopathy, *SD* standard deviation
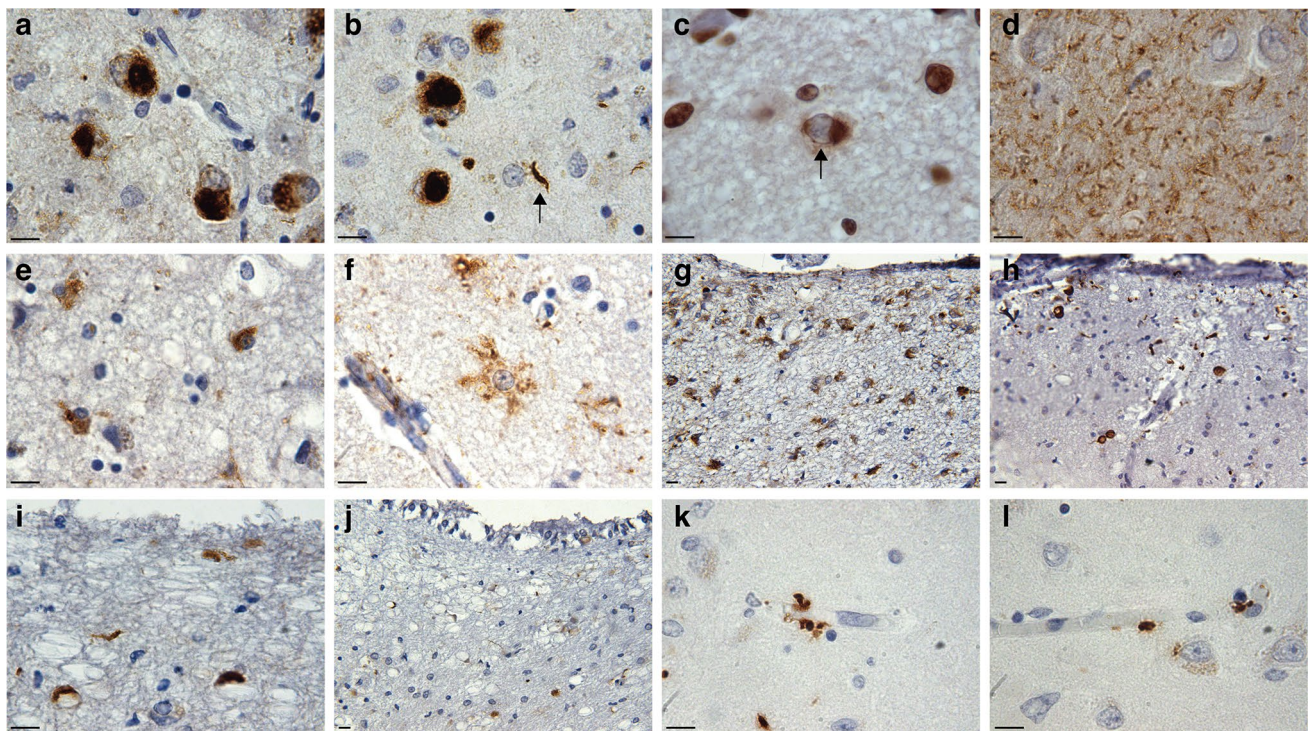
Fig. 1 Pathologic features of TDP-43 immunohistochemistry in BLSA cohort. **a** TDP-43+ neuronal cytoplasmic inclusions (NCIs) (phosphorylation dependent TDP-43 antibody). **b** TDP-43+ NCIs and neurites (arrow) (phosphorylation dependent TDP-43 antibody). **c** TDP-43 nuclear clearance (arrow) and cytoplasmic inclusion by phosphorylation-independent TDP-43 antibody. **d** Dense networks of TDP-43+ neurites (phosphorylation dependent TDP-43 antibody). **e–g** TDP-43+ glial cells, including oligodendrocytes (**e**), astrocytes (**f**), and astrocytes with ARTAG-like pattern (**g**) (phosphorylation dependent TDP-43 antibody). **h–j** TDP-43+ cell processes in subpial region and subependymal region (phosphorylation dependent TDP-43 antibody), usually associated with abundant corpora amylacea. **k**, **l** perivascular TDP-43+ pattern (phosphorylation dependent TDP-43 antibody). Scale bars, 10 μm

TDP-43 with nuclear clearance only, none had perivascular TDP-43 pathology. For total of 122 brains without TDP-43 pathology, only 2 (1.6%) had perivascular TDP-43 pathology. Sections of precuneus and inferior parietal lobule were stained in randomly selected cases (n = 22) encompassing all LATE-NC stages. Only 4 of the 22 brains revealed TDP-43 lesions. One LATE-NC stage 2 case had TDP-43+ NCIs and neurites in both precuneus and inferior parietal lobule. Another LATE-NC stage 2 case had one TDP-43+ NCI and few neurites in the inferior parietal lobule, while two additional LATE-NC stage 2 cases had only rare TDP-43+ neurites in the inferior parietal lobule.

The participants with LATE-NC have older mean age of death than the TDP-43 negative group (91.3 vs. 86.8 years, *p* < 0.001) (Table 1). The frequency of LATE-NC increases with age (Fig. 2a), is higher in females than males (52.1% vs. 29.5%, *p* < 0.001) (Fig. 2b), but not significantly different in APOE ε4 carriers as compared

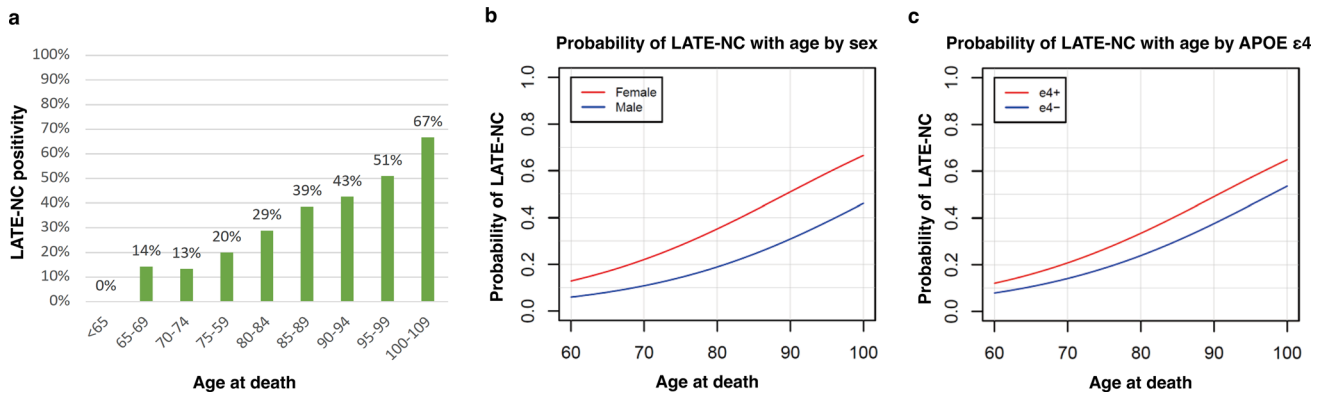**Fig. 2** Limbic-predominant age-related TDP-43 encephalopathy neuropathologic change (LATE-NC) positivity with age, sex, APOE ε4 status. **a** The frequency of LATE-NC increases with age at death. **b** Predicted probability of LATE-NC positivity increases 6.7% per year and is higher in females. Being female increases the odds of LATE-NC by 2.33-fold ($p = 0.0014$). **c** The APOE ε4 allele increases the probability of LATE-NC by 60.7% but does not reach statistical significance at 0.05 level ($p = 0.1052$). Results are not adjusted for covariates (also see Table 2)

Table 2 Relation of age, sex, and APOE ε4 with LATE-NC by logistic regression

Predictor	Outcome: LATE-NC positivity		
	OR	95% CI	*p* value
Age	1.067	(1.031, 1.105)	**0.0002**
Sex	0.429	(0.256, 0.721)	**0.0014**
APOE ε4	1.607	(0.906, 2.826)	0.1052

Significant *p* values are bolded

LATE-NC limbic-predominant age-related TDP-43 encephalopathy neuropathologic change, *OR* odds ratio, *95% CI* 95% confident interval

to non-APOE ε4 carriers (45.3% vs. 34.4%, $p = 0.126$) (Fig. 2c). To investigate the effects of age, sex, and APOE ε4 status on the probability of LATE-NC presence, we used logistic regression analysis with LATE-NC as the outcome. None of the interaction terms is significant in the logistic regression model relating age, sex, and APOE ε4 with the probability of LATE-NC. The final model included the main effects of age, sex and APOE ε4, and this model has c statistics (AUC) of 0.695. Age at death and female sex are significantly predictive of LATE-NC ($p = 0.0002$ and $p = 0.0014$, respectively; Fig. 2b, Table 2). Every year increment increased the odds of being positive by 6.7%. Being female increased the odds of LATE-NC by 2.33-fold. Although APOE ε4 increased the odds of LATE-NC positivity by 60.7%, it did not reach statistical significance at 0.05 level. Results are not adjusted for other covariates. (Fig. 2c, Table 2).

Association of LATE-NC with Alzheimer's disease neuropathologic changes

The frequency of LATE-NC increases with higher CERAD NP scores and Braak NFT stages (Fig. 3) [10, 59]. After adjusting for age at death, sex, and APOE ε4 status, both CERAD NP score and Braak NFT stage are significantly associated with probability of LATE-NC from logistic regression models ($p = 0.0008$ and < 0.0001, respectively; Table 3); and each unit increase in CERAD NP score and Braak NFT stage is associated with a 57% and 58% increase in odds of LATE-NC, respectively (Table 3, Supplementary Table 1 and 2). Due to higher frequency of LATE-NC in females compared to males, we further examined the relationship between sex and ADNC by a regression model. After adjusting for age at death and APOE ε4 status, males had lower CERAD NP score (beta = − 0.296, standard error = 0.131, $p = 0.024$) and Braak score (beta = − 0.540, standard error = 0.157, $p = 0.0007$) compared with females.

LATE-NC and domain-specific cognitive decline

Participants of the BLSA cohort underwent comprehensive longitudinal cognitive assessments. The characteristics of the longitudinal cognitive sample are in Supplementary Table 3. Out of the total 309 participants, 243 participants who had complete longitudinal cognitive assessments were included in the analysis of cognitive decline. We used separate linear mixed effects models with each longitudinal cognitive measure as the outcome, and sex and age at death as covariates in the first set of models. The effects of LATE-NC on longitudinal trajectories of CVLT immediate recall (verbal memory) and Card Rotations Test (visuospatial ability) are highly significant in the first models (CVLT
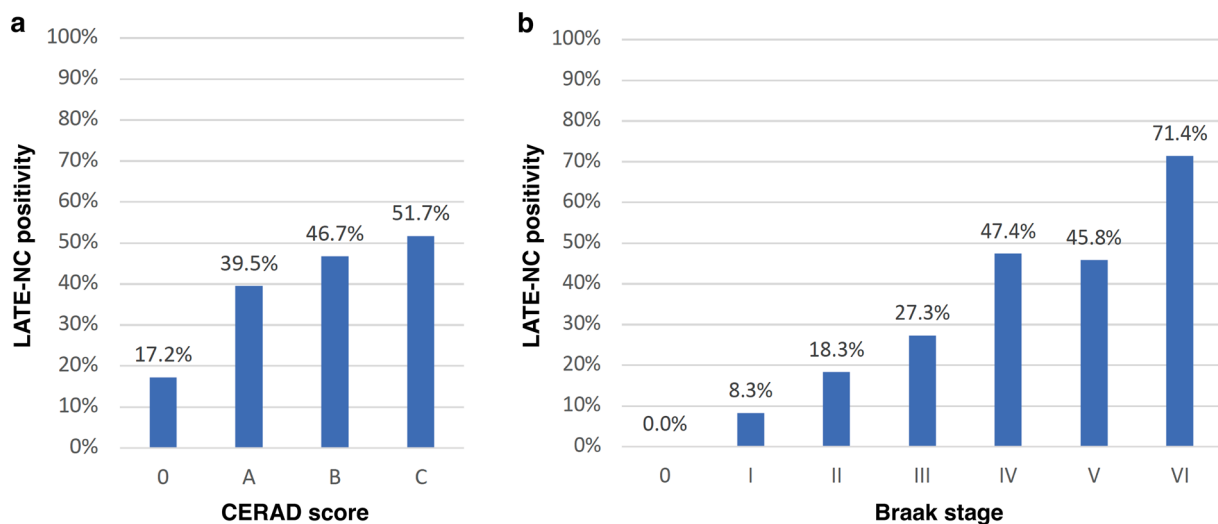
Fig. 3 Limbic-predominant age-related TDP-43 encephalopathy neuropathologic change (LATE-NC) positivity with CERAD neuritic plaques (NP) score and Braak neurofibrillary tangles (NFT) stage. **a** The frequency of LATE-NC positivity increases with higher CERAD NP scores. **b** The frequency of LATE-NC positivity increases with higher Braak NFT stages. By logistic regression models, there are significant association between the LATE-NC positivity with both CERAD NP score (see Table 3 and Supplementary Table 1) and Braak NFT stage (see Table 3 and Supplementary Table 2)

Table 3 Relation of CERAD NP score and Braak NFT stage with LATE-NC

Predictor	Outcome: LATE-NC positivity					
	Model 1 (without adjusting covariates)			Model 2 (adjusting for age at death, sex, and APOE ε4)		
	OR	95% CI	*p* value	OR	95% CI	*p* value
CERAD NP score	1.721	(1.366, 2.167)	**< 0.0001**	1.569*	(1.207, 2.039)	**0.0008**
Braak NFT stage	1.831	(1.495, 2.244)	**< 0.0001**	1.583**	(1.264, 1.984)	**< 0.0001**

Significant *p* values are bolded

LATE-NC Limbic-predominant age-related TDP-43 encephalopathy neuropathologic change, *NP* neuritic plaques, *NFT* neurofibrillary tangles, *OR* odds ratio, *95% CI* 95% confident interval

*Corresponds to 57% increase and **to 58% increase

immediate recall $p = 0.0001$, Card Rotations Test $p < 0.0001$; Fig. 4a, b, Table 4). Both tests showed significant differences in scores between LATE-NC positive and negative groups. The difference estimates for CVLT immediate recall scores are − 13.40 at 1 year prior to death ($p < 0.0001$), − 8.94 at 5 years prior to death ($p < 0.0001$), and − 4.41 at 10 years prior to death ($p = 0.0124$). The difference estimates for Card Rotations Test scores are − 13.62 at 1 year prior to death ($p = 0.0135$), − 12.28 at 5 years prior to death ($p = 0.0018$), and − 7.68 at 10 years prior to death ($p = 0.0709$). The effects of LATE-NC positivity on longitudinal slopes of MMSE and Category Fluency Test are also significant ($p = 0.039$ and $p = 0.026$, respectively) in the first model (Fig. 4c, d, Table 4). The differences in MMSE and Category Fluency Test scores between LATE-NC positive and negative groups are also significant. The difference estimates of MMSE and Category Fluency Test scores are − 1.87 and − 2.05 at 1 year

prior to death ($p = 0.0054$ and 0.0044, respectively), − 1.42 and − 1.45 at 5 years prior to death ($p = 0.0016$ and 0.0048, respectively), and − 0.86 and − 0.81 at 10 years prior to death ($p = 0.0023$ and 0.0092, respectively). After adding CERAD NP score and Braak NFT stage as covariates, the effects of LATE-NC on longitudinal trajectories of CVLT immediate recall and Card Rotations Test remain significant (CVLT immediate recall $p = 0.0048$, Card Rotations Test $p = 0.0007$). However, the effects on the longitudinal slopes of MMSE and Category Fluency Test are no longer significant ($p = 0.286$ and $p = 0.183$, Table 4). The effects of LATE-NC on the longitudinal trajectories and levels of cognitive measures of Trail Making Test A, Trail Making Test B, Trail Making Test B-A, and Letter fluency test are not significant. In summary, LATE-NC has significant effects on verbal memory (CVLT immediate recall), visuo-spatial ability (Card Rotations Test), mental status (MMSE)

Fig. 4 Longitudinal trajectories of cognitive function in different domains. The effects of Limbic-predominant age-related TDP-43 encephalopathy neuropathologic change (LATE-NC) on longitudinal trajectories of CVLT immediate recall (verbal memory) (**a**) and Card Rotations Test (visuospatial ability) (**b**) are highly significant. The differences in MMSE (**c**) and Category Fluency Test (**d**) trajectories between LATE-NC positive and negative groups are also significant
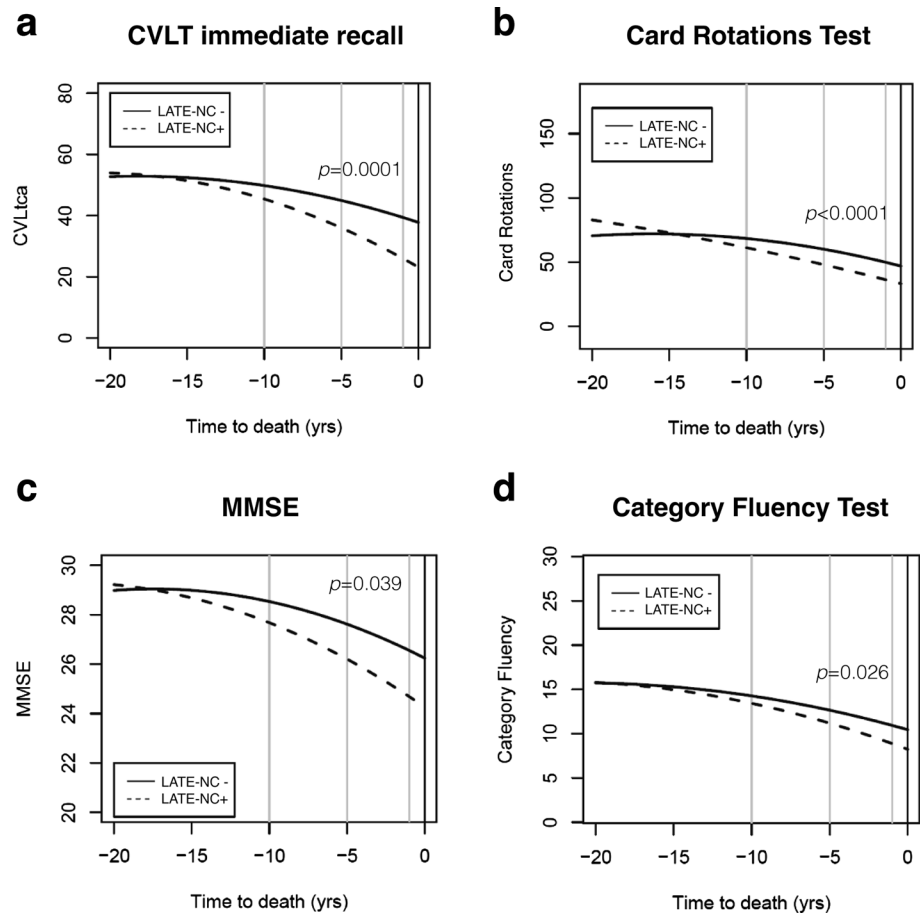
and semantic fluency (Category Fluency Test). Notably, the effects of LATE-NC on verbal memory and visuospatial ability remain significant after adjusting for ADNC. However, LATE-NC does not significantly affect attention, executive function (Trail Making Tests) or phonemic fluency (Letter Fluency Test).

TDP-43 nuclear clearance: an early marker of TDP-43 proteinopathy

Under normal circumstances, TDP-43 is localized in the nucleus of neurons, a feature demonstrated using a phosphorylation independent TDP-43 antibody (Figs. 1c and 5d). By contrast, TDP-43 proteinopathy is characterized by a triad of TDP-43+ cytoplasmic and neuritic inclusions (NCI) plus nuclear clearance. There is growing evidence suggesting that TDP-43 nuclear clearance, in the absence of NCI, is sufficient to cause loss of function of TDP-43 in neurons, and it is likely an early event of TDP-43 proteinopathy [66, 81, 87]. We examined this notion by evaluating TDP-43 immunohistochemistry (IHC) in the dentate gyrus of the hippocampus with a phosphorylation independent TDP-43 antibody in all subjects in the BLSA cohort. Only cells with neuronal morphology were evaluated. Triple immunofluorescent labeling

with phosphorylation independent and phosphorylation dependent TDP-43 antibodies, and neuronal marker NeuN was performed to assess nuclear clearance of TDP-43 as well as NCI (Fig. 5a–c). Results defined three distinct groups: (1) no TDP-43 pathology (n = 147, 47.6%), (2) presence of both TDP-43+ NCIs with nuclear clearance of TDP-43 (n = 118, 38.2%), and (3) presence of TDP-43 nuclear clearance only without TDP-43+ NCIs (n = 44, 14.2%). Remarkably, the mean age of participants in the TDP-43 nuclear clearance only group is younger than the TDP-43+ NCIs group (86.7 vs. 91.3, $p = 0.002$). Comparison of TDP-43 nuclear clearance only group and no TDP-43 pathology group showed that the TDP-43 nuclear clearance only group has higher rate of APOE ε4 (36.6% vs. 18.8%, p = 0.033; Table 5). The effects of TDP-43 nuclear clearance in absence of NCI on the longitudinal trajectories and levels of cognitive measures are not significant (Table 6, Supplementary Table 4).

Because the age of death of participants in BLSA cohort was ≥ 57 years of age (mean 88.5 years), we examined the autopsy brain of 24 younger individuals aged 20 to 60 years (mean age 43 years). Among these 24 brains, 4 (16.7%) had low-level ADNC, 6 (25%) had primary aging related tauopathy (PART), and 14 (58.3%) were normal. Their demographic and clinico-pathological characteristics are

Table 4 LATE-NC effects on cognitive domains

Outcome			Model 1 Sex age at death adjusted	Model 2 Sex age at death CERAD score Braak stage adjusted
CVLT immediate recall	LATE-NC on cognitive trajectory		**p = 0.0001**	**p = 0.0048**
	Cognitive difference at year(s) prior to death Estimate (SE) *p* value	1 year	− 13.40 (2.98) **p < 0.0001**	− 10.42 (2.99) **p = 0.0005**
		5 years	− 8.94 (2.02) **p < 0.0001**	− 7.11 (2.06) **p = 0.0006**
		10 years	− 4.41 (1.76) **p = 0.0124**	− 3.70 (1.81) **p = 0.0409**
Card Rotations Test	LATE-NC on cognitive trajectory		**p < 0.0001**	**p = 0.0007**
	Cognitive difference at year(s) prior to death Estimate (SE) *p* value	1 year	− 13.62 (5.49) **p = 0.0135**	− 10.32 (5.70) p = 0.0707
		5 years	− 12.28 (4.23) **p = 0.0018**	− 9.14 (4.42) **p = 0.0392**
		10 years	− 7.68 (4.24) p = 0.0709	− 4.98 (4.39) p = 0.256
MMSE	LATE-NC on cognitive trajectory		**p = 0.039**	p = 0.286
	Cognitive difference at year(s) prior to death Estimate (SE) *p* value	1 year	− 1.87 (0.67) **p = 0.0054**	na
		5 years	− 1.42 (0.45) **p = 0.0016**	na
		10 years	− 0.86 (0.28) **p = 0.0023**	na
Category Fluency Test	LATE-NC on cognitive trajectory		**p = 0.026**	p = 0.183
	Cognitive difference at year(s) prior to death Estimate (SE) *p* value	1 year	− 2.05 (0.72) **p = 0.0044**	na
		5 years	− 1.45 (0.51) **p = 0.0048**	na
		10 years	− 0.81 (0.48) p = 0.092	na
Letter Fluency Test	LATE-NC on cognitive trajectory		p = 0.13	
Trail-Making A	LATE-NC on cognitive trajectory		p = 0.43	
Trail-Making B	LATE-NC on cognitive trajectory		p = 0.86	
Trail-Making B-A	LATE-NC on cognitive trajectory		p = 0.92	

Significant *p* values are bolded

LATE-NC Limbic-predominant age-related TDP-43 encephalopathy neuropathologic change, *SE* standard error

summarized in Table 7. TDP-43 nuclear clearance without TDP-43+ NCIs was first noted in the 50 s, while the TDP-43+ NCIs appeared in the 60 s (Fig. 5e, Supplementary Table 5). We did not find any brains with TDP-43 nuclear clearance in brains younger than 50 years old. In summary, TDP-43 nuclear clearance precedes the onset of TDP-43+ NCIs by approximately a decade.

Cryptic exon RNA and protein detection

TDP-43 represses the splicing of cryptic exons and loss of this function has been proposed to be an important mechanism of TDP-43 associated proteinopathy and neurodegeneration [13, 46, 50, 52, 57, 75]. To assess for TDP-43 splicing

repression, we used BaseScope RNA in situ hybridization with an RNA probe targeting a cryptic exon in *Hepatoma-Derived Growth Factor-Like 2* (*HDGFL2*) transcript in 5 brains with TDP-43+ NCIs, 5 brains with TDP-43 nuclear clearance only, and 5 brains without TDP-43 pathology. All 5 cases (100%) with TDP-43+ NCIs and all 5 cases (100%) with TDP-43 nuclear clearance only revealed cryptic HDGFL2 RNA transcripts (Fig. 6a, b, 7b, d). All five brains without TDP-43 pathology were negative for cryptic *HDGFL2* RNA transcript (Fig. 6c). The quantification of cryptic *HDGFL2* RNA transcripts revealed that brains with TDP-43+ NCIs had an average of 260.5 per 1000 cells (median: 197 per 1000 cells) (Fig. 6d). Brains with TDP-43 nuclear clearance only had an average of 174.7 per 1000
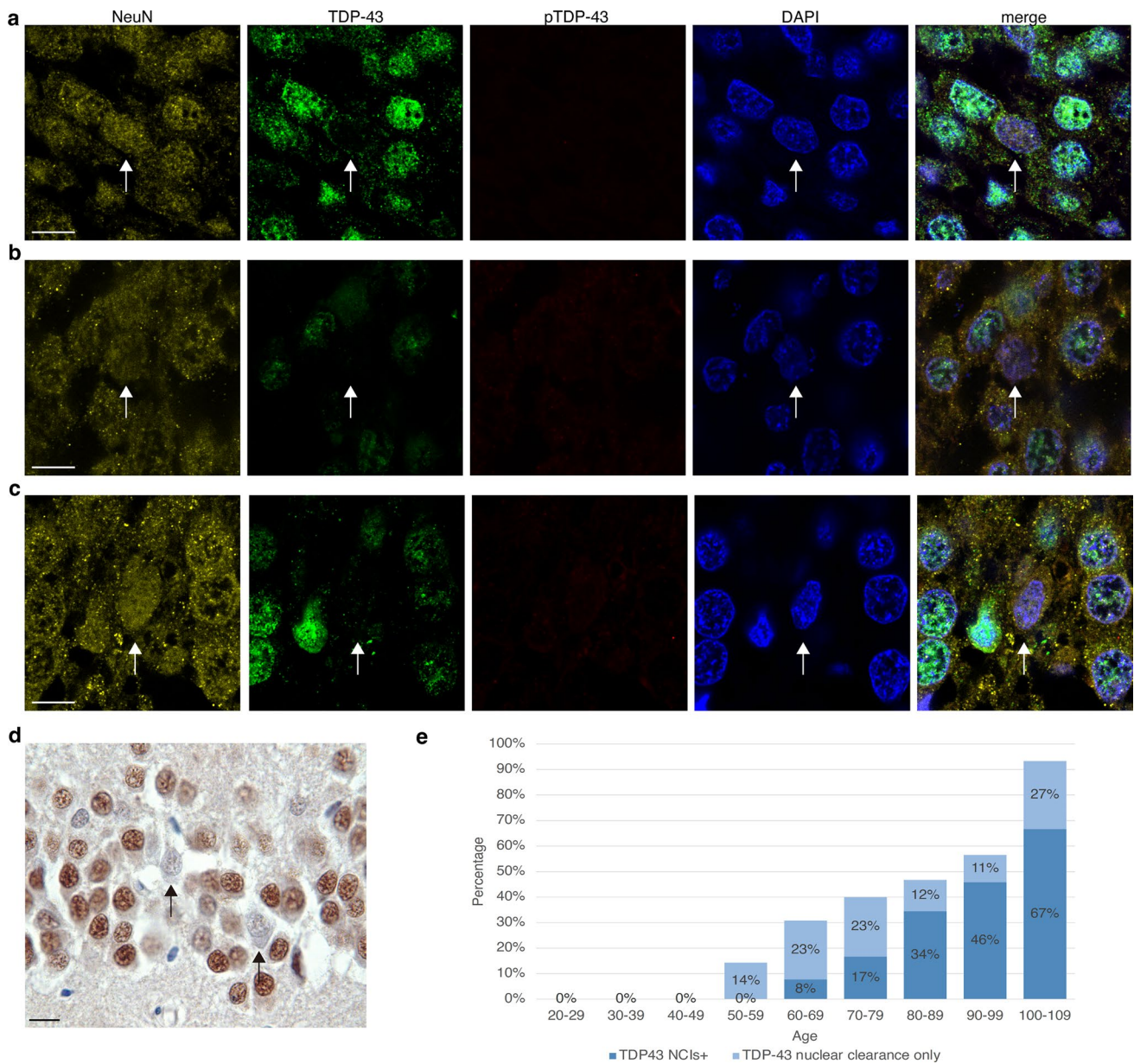
Fig. 5 Nuclear clearance of TDP-43 in dentate gyrus of the hippocampus. **a–c** Three representative cases of TDP-43 nuclear clearance without TDP-43+ neuronal cytoplasmic inclusions (NCIs). Immunofluorescent stains with neuronal marker (NeuN), phosphorylation-independent TDP-43 (TDP-43), phosphorylation-dependent TDP-43 (pTDP-43), and DNA stain with DAPI revealed some neurons (white arrow) have loss of nuclear TDP-43 but no TDP-43+ NCIs on either by phosphorylation-dependent TDP-43 and phosphorylation-independent TDP-43 stains. **d** The immunoperoxidase stain with phosphorylation-independent TDP-43 antibody showed loss of TDP-43 staining in the nuclei of the granule cells (arrows) but no TDP-43+ NCIs. **e** Age distribution of TDP-43 nuclear clearance only and TDP-43+ NCIs in the BLSA and younger autopsy cohorts. Scale bars, 10 μm

cells (median: 166 per 1000 cells) (Fig. 6d). Brains without TDP-43 pathology had an average of 12.2 per 1000 cells (median: 13 per 1000 cells), which was considered background signal. Both brains with TDP-43+ NCIs and brains with TDP-43 nuclear clearance only showed significantly higher numbers of cryptic *HDGFL2* transcripts compared to brains without TDP-43 pathology (Mann–Whitney test, $p < 0.01$ for both comparisons) (Fig. 6d). No significant difference in levels of cryptic *HDGFL2* transcripts was observed between brains with TDP-43+ NCIs compared to those with TDP-43 nuclear clearance only (Mann–Whitney test, $p = 0.15$).

We then used a monoclonal antibody recognizing the cryptic exon-encoded neoepitope in HDGFL2 to corroborate its cryptic exon inclusion (Supplementary Information) [35]. Cryptic HDGFL2 IF staining was performed

Table 5 Clinico-pathologic characteristics of cases with TDP-43 nuclear clearance only vs. no TDP-43 pathology in the BLSA cohort

Characteristics	TDP-43 nuclear clearance only	No TDP-43 pathology	p value
Case number	44	147	
Age at death			
Mean (SD)	86.7 (11.2)	86.8 (8.1)	0.968
Range	57.6–103.1	62.9–109.5	
Sex			0.134
Male	27 (61.4%)	108 (73.5%)	
Female	17 (38.6%)	39 (26.5%)	
Race			0.709
White	39 (88.6%)	136 (92.5%)	
African–American	3 (6.8%)	7 (4.8%)	
Other	2 (4.5%)	4 (2.7%)	
CERAD NP score [59]			0.426
0	15 (34.1%)	57 (38.8%)	
A	3 (6.8%)	20 (13.6%)	
B	19 (43.2%)	46 (31.3%)	
C	7 (15.9%)	21 (14.3%)	
Braak NFT stage [10]			0.814
0	1 (2.3%)	3 (2.0%)	
I	2 (4.5%)	9 (6.1%)	
II	9 (20.5%)	40 (27.2%)	
III	10 (22.7%)	30 (20.4%)	
IV	17 (38.6%)	43 (29.3%)	
V	2 (4.5%)	11 (7.5%)	
VI	3 (6.8%)	7 (4.8%)	
APOE ε4 carrier			**0.033**
ε4 carrier	15 (36.6%)	26 (18.8%)	
Non-ε4 carrier	26 (63.4%)	122 (81.2%)	
Cognitive function			0.190
Normal	20 (45.5%)	66 (45.2%)	
MCI	11 (25.0%)	21 (14.4%)	
Dementia	13 (29.5%)	59 (40.4%)	

Significant *p* values are bolded

NFT neurofibrillary tangles, *NP* neuritic plaques, *SD* standard deviation

in 6 brains with TDP-43+ NCIs, 10 brains with TDP-43 nuclear clearance only, and 6 brains without TDP-43 pathology. All 6 (100%) brains with TDP-43+ NCIs were positive for cryptic HDGFL2 accumulation (Fig. 7a). Among brains with TDP-43 nuclear clearance only, 4 out of 10 (40%) had positive cryptic HDGFL2 accumulation (Fig. 7c). All 6 brains without TDP-43 pathology were negative for cryptic HDGFL2 staining. A peptide competition study was conducted to ascertain the specificity of the cryptic HDGFL2 antibody. Three different peptides, each possessing amino acid sequences derived from the cryptic peptide within HDGFL2, were tested. The peptide bearing the C-terminal of the cryptic HDGFL2 peptide effectively blocked the staining of the cryptic HDGFL2 antibody, whereas the other two peptides failed to block the cryptic HDGFL2 antibody staining (Fig. 8). Together, these data suggest that during aging loss of TDP-43 splicing repression occurs initially in neurons depleted of nuclear TDP-43 lacking NCI, supporting the notion that such loss contributes to the progression of disease or exacerbates neurodegeneration and cognitive decline in mixed etiology dementia harboring TDP-43 pathology.

Association of TDP-43 nuclear clearance and tau pathology

TDP-43 proteinopathy is associated with increased tau pathology in patients with AD, even in cases lacking high Braak NFT stages [58, 80, 85]. We examined the tau pathology in dentate gyrus of the hippocampus in brains from three TDP-43 pathology groups: brains with TDP-43+ NCIs, brains with TDP-43 nuclear clearance only, and brains without TDP-43 pathology. Subsets of brains from Braak NFT stage 0-III or Braak NFT stage V/VI with similar CERAD NP scores and Braak NFT stages within each group were selected. There were no significant differences in the average CERAD NP scores and Braak NFT stages between three TDP-43 pathology groups (Supplementary Table 6 and Supplementary Table 7), confirmed by Kruskal–Wallis tests ($p = 0.452$ for CERAD NP scores and $p = 0.437$ for Braak NFT stages for Braak NFT stage 0-III; $p = 0.764$ for CERAD NP scores and $p = 0.670$ for Braak NFT stages for Braak NFT stage V/VI). We identified increased tau-positive granule cells in the dentate gyrus from brains with TDP-43 NCIs and TDP-43 nuclear clearance only (Fig. 9a). Brains with TDP-43+ NCIs had a significant higher number of tau-positive granule cells compared to brains with no TDP-43 pathology in both Braak NFT stage 0-III group and Braak NFT stage V/VI group ($p < 0.0001$ for Braak NFT stage 0-III, and $p = 0.0147$ for Braak NFT stage V/VI, Fig. 9b, Supplementary Table 8–10). Importantly, brains with TDP-43 nuclear clearance only also showed a significant higher number of tau-positive granule cells compared to brains with no TDP-43 pathology in both Braak NFT stage 0-III group and Braak NFT stage V/VI group ($p = 0.0243$ for Braak NFT stage 0-III, and $p = 0.028$ for Braak NFT stage V/VI, Fig. 9b, Supplementary Table 8–10). Taken together, these results support the idea that loss of TDP-43 splicing repression exacerbates tau pathology to accelerate neurodegeneration and cognitive decline in cases of ADNC.

Table 6 TDP-43 nuclear clearance effects on cognitive domains

Outcome		Model 1 Sex & age at death adjusted	Model 2 Sex age at death CERAD score & Braak stage adjusted
CVLT immediate recall	TDP-43 nuclear clearance on cognitive trajectory	$p = 0.345$	$p = 0.403$
	Cognitive difference at 1 year prior to death Estimate (SE) p value	− 0.76 (3.39) $p = 0.823$	− 1.10 (3.28) $p = 0.73$
Card Rotations Test	TDP-43 nuclear clearance on cognitive trajectory	$p = 0.853$	$p = 0.855$
	Cognitive difference at 1 year prior to death Estimate (SE) p value	5.63 (7.37) $p = 0.446$	4.61 (7.44) $p = 0.536$
MMSE	TDP-43 nuclear clearance on cognitive trajectory	$p = 0.937$	$p = 0.973$
	Cognitive difference at 1 year prior to death Estimate (SE) p value	0.168 (0.615) $p = 0.785$	0.146 (0.602) $p = 0.809$
Category Fluency Test	TDP-43 nuclear clearance on cognitive trajectory	$p = 0.824$	$p = 0.945$
	Cognitive difference at 1 year prior to death Estimate (SE) p value	− 0.776 (0.974) $p = 0.426$	− 0.749 (0.960) $p = 0.436$

SE standard error

Table 7 Demographics and clinico-pathologic characteristics of individuals from the younger autopsy cohort (n = 24)

Characteristics	Total
Case number	24
Age at death	
Mean (SD)	43.0 (13.5)
Range	21–68
Sex	
Male	21 (87.5%)
Female	3 (12.5%)
Race	
White	18 (75.0%)
African–American	4 (16.7%)
Others	2 (8.3%)
Clinical diagnosis	
Drug or alcohol abuse	15 (62.5%)
Cardiovascular disease	4 (16.7%)
Intoxication	1 (4.2%)
Others or unknown	4 (16.7%)
Neuropathologic diagnosis	
ADNC low level	4 (16.7%)
PART	6 (25.0%)
Normal	14 (58.3%)

ADNC Alzheimer's disease neuropathologic change, *PART* primary aging-related tauopathy, *SD* standard deviation

Discussion

This clinico-pathological study of more than 300 BLSA participants shows that LATE-NC is present in 38.2% of the cohort, it frequently coexists with ADNC, and is associated with domain-specific cognitive decline in the aging population. Although LATE-NC is associated with higher levels of ADNC, our results reveal that TDP-43 proteinopathy has clinical impacts on verbal memory and visuospatial function which are independent from the ADNC. This observation suggests that TDP-43 proteinopathy and canonical pathology of Alzheimer's disease impacts different pathogenic processes in the aging brain. Thus, TDP-43 proteinopathy should be considered as one of several key independent factors that contributes and interacts with other pathogenic pathways underlying cognitive decline in the aging population.

Our study shows that the prevalence of TDP-43 proteinopathy and LATE-NC is higher in cases with higher CERAD NP score and Braak NFT stage, similar to a recent study that collected data from 13 different cohorts [68]. Our study also shows a higher frequency of LATE-NC in females independent of age or APOE status. This higher frequency could be associated with higher CERAD NP scores and Braak NFT stages in females in our cohort. Some previous studies have also shown higher ADNC pathology scores in females [24, 32], but the presence of a greater frequency of LATE-NC in females has not been previously addressed. Some previous studies have shown an association between APOE ε4 allele and LATE-NC [16, 21, 39, 40, 94], while
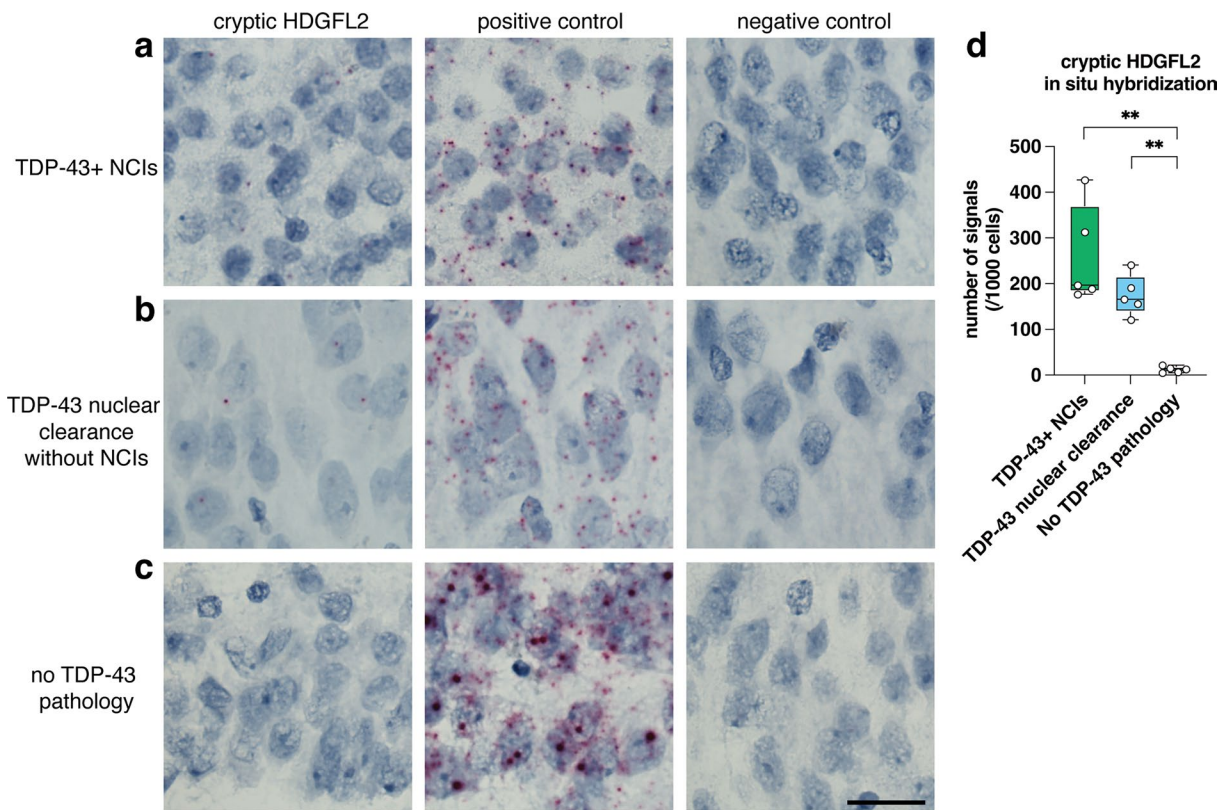
Fig. 6 RNA in situ hybridization using a probe targeting cryptic HDGFL2 transcripts. **a** Cryptic HDGFL2 RNA in situ hybridization shows positive cryptic HDGFL2 labeling in a case with TDP-43+ NCIs. **b** Cryptic HDGFL2 RNA in situ hybridization shows positive cryptic HDGFL2 labeling in a case with TDP-43 nuclear clearance without TDP-43+ NCIs. **c** Cryptic HDGFL2 RNA in situ hybridization is negative in a case with no TDP-43 pathology. In all cases, the positive control probe (ubiquitin C) shows prominent labeling, and the negative control shows no signal (**a**–**c**). Scale bar, 25 μm. **d** Quantification of cryptic HDGFL2 transcripts showed higher numbers of cryptic HDGFL2 transcripts in TDP-43+ NCIs group and TDP-43 nuclear clearance only group compared to no TDP-43 pathology group. $*p < 0.05$, $**p < 0.01$
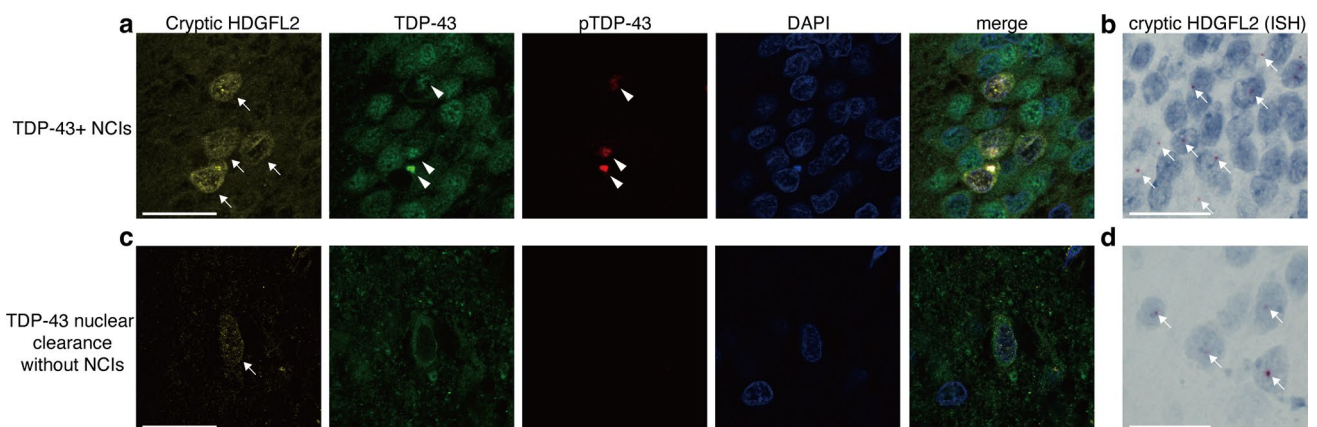
Fig. 7 Cryptic HDGFL2 protein and RNA transcript detection in cases with TDP-43+ NCIs (**a**, **b**) and TDP-43 nuclear clearance only (**c**, **d**). Immunofluorescent stains with antibody against cryptic HDGFL2 peptide, phosphorylation-independent TDP-43 (TDP-43), phosphorylation-dependent TDP-43 (pTDP-43), and DAPI for DNA stain. **a** presence of cryptic peptide in neuronal nucleus and peri-karyon (arrows) and TDP-43+ NCIs (arrowheads). **b** positive cryptic HDGFL2 RNA in situ hybridization (arrows) in the same brain as in a. **c** presence of cryptic peptide (arrow) and absence of nuclear TDP-43. **d** positive cryptic HDGFL2 RNA in situ hybridization (arrows) in the same brain as in **c**. Scale bars, 25 μm
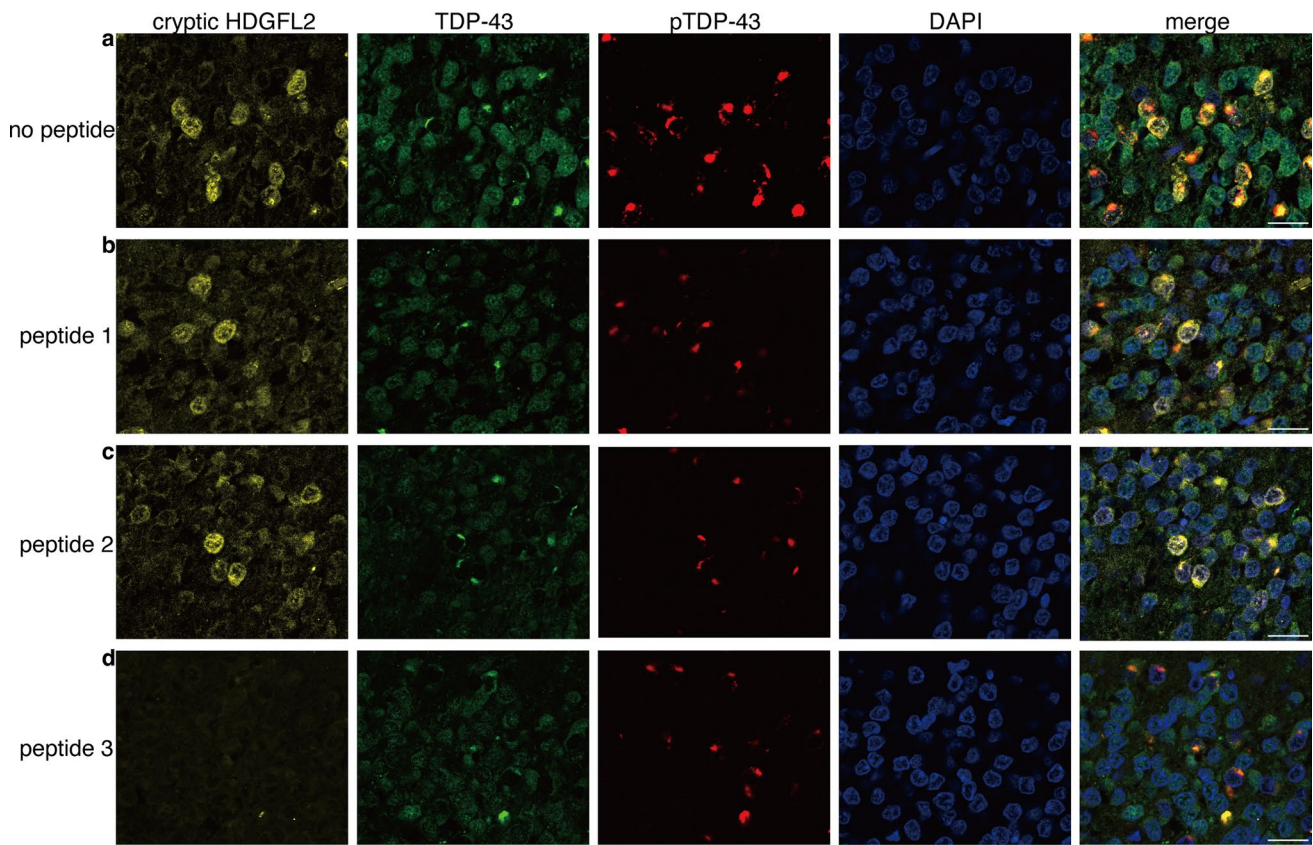
Fig. 8 Peptide competition study for cryptic HDGFL2 antibody demonstrating block of staining by peptide 3. **a** Immunofluorescent stains of cryptic HDGFL2, phosphorylation-independent TDP-43 (TDP-43), phosphorylation-dependent TDP-43 (pTDP-43), and DNA stain with DAPI reveals cryptic HDGFL2 expression in cells with TDP-43+NCIs. **b**, **c** the cryptic HDGFL2 antibody staining is not blocked by peptide 1 or peptide 2. **d** peptide 3 completely blocks the cryptic HDGFL2 antibody staining. Scale bars, 20 μm
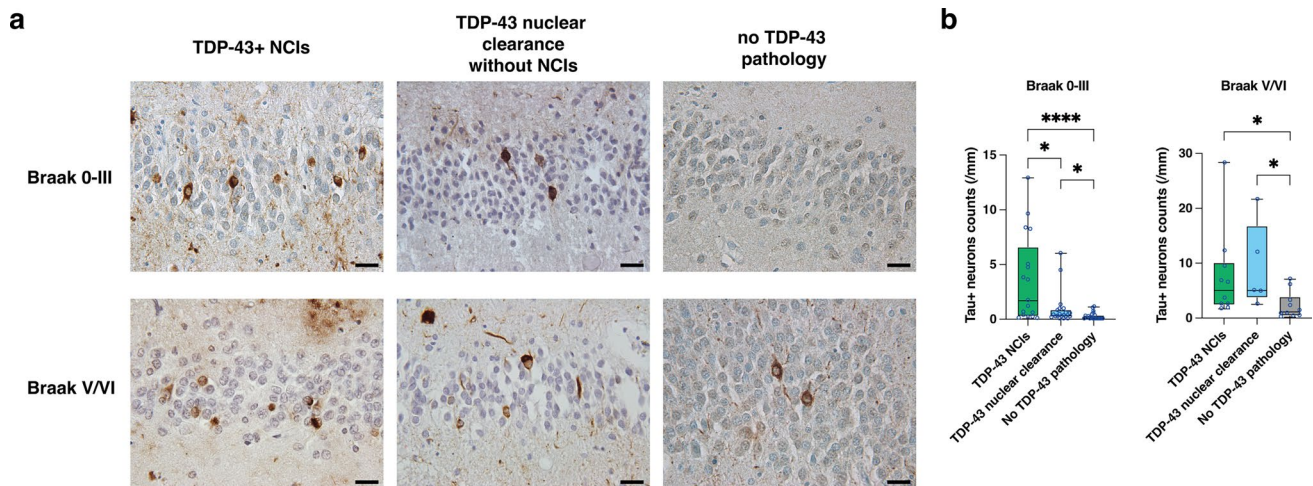
Fig. 9 Increased tau pathology in dentate gyrus in brains with TDP-43+NCIs and brains with TDP-43 nuclear clearance. **a** Immunohistochemical stains of phospho-tau (AT8) showed increased tau pathology in the dentate gyrus in brains with TDP-43+NCIs and TDP-43 nuclear clearance. **b** Quantification of number of tau-positive granule cells in dentate gyrus showed significant higher number in brains with TDP-43 NCIs and TDP-43 nuclear clearance compared to brains with no TDP-43 pathology in both Braak NFT stage 0-III and Braak NFT stage V/VI groups. Scale bar, 25 μm; $*p < 0.05$, $**p < 0.01$, $***p < 0.001$, $****p < 0.0001$

other studies have failed to demonstrate this association [14, 28, 29, 78, 88]. In our study, we observed a statistically significant relationship between the APOE ε4 allele and TDP-43 nuclear clearance. Although the APOE ε4 allele increased the probability of TDP-43 NCIs, this relationship did not reach statistical significance. This may be attributed to an insufficient sample size.

The longitudinal trajectories of cognitive function in our study show that LATE-NC was associated with faster rates of cognitive decline in verbal episodic memory (California Verbal Learning Test (CVLT) immediate recall), visuospatial ability (Card Rotations Test), mental status (MMSE) and semantic fluency (Category Fluency Test). The CVLT immediate recall and Card Rotations Test scores show large differences between participants with and without LATE-NC. Both test results have more than 13-point differences at 1 year prior to death. By contrast, the differences in MMSE and Category Fluency Test are smaller. Several lines of evidence indicate that NPs in AD are associated with rate of cognitive decline, and that NFTs are also associated with cognitive impairment in both AD patients and non-AD patients with PART [5, 6, 19, 37, 53, 60]. Therefore, we used both CERAD NP score and Braak NFT stage as covariates to adjust for effects of ADNC severity in our analysis of cognitive decline, demonstrating that effects of TDP-43 loss on decline of verbal memory and visuospatial ability were independent of ADNC. By contrast, most previous studies of LATE-NC and cognitive decline have not included CERAD NP score or Braak NFT stage as covariates, limiting the assessment of the separate contributions of TDP-43 proteinopathy and ADNC to cognitive decline. We confirmed the impact of TDP-43 proteinopathy on verbal episodic memory decline, already shown by some previous studies [44, 92]. In addition, our study is the first to show that cases with TDP-43 proteinopathy have significant decline in visuo-spatial ability independent of ADNC. The impairment of visuo-spatial ability is frequently seen in patients with Alzheimer's dementia and often occurs in early stages [38, 89]. Many brain cortical regions are involved in visuo-spatial ability, including occipital lobe, parietal lobe, prefrontal cortex, premotor cortex, inferior temporal cortex, and mesial temporal lobe [47]. The parietal lobe, especially posterior parietal cortex which includes superior parietal lobule, inferior parietal lobule and intraparietal sulcus, is important for visuospatial processing [30, 47, 93]. The precuneus has strong functional connectivity with the angular gyrus and is important for visuospatial processing in humans [8, 47]. In Alzheimer's disease, several studies have shown that early amyloid deposition occurs in the precuneus during preclinical stages [4, 20], but no prior study has examined the TDP-43 pathology in this region. To examine LATE-NC in the parietal lobe and precuneus, we randomly selected 22 brains spanning the whole range of LATE-NC stages. We found 4

of 22 cases had TDP-43 pathology in inferior parietal lobule or precuneus, and the burden of TDP-43 pathology in these cases is quite low. By contrast, the mesial temporal structures uniformly bear LATE-NC. These structures are part of the parieto-medial temporal pathway that subserves visuo-spatial processing in humans and is important in navigation, topographic and spatial learning [47] and the hippocampus plays an important role in allocentric spatial memory formation in human [73, 82]. This pathway is also important in the decline of visuo-spatial ability in patients with Alzheimer's disease [47, 48, 95]. Therefore, loss of TDP-43 splicing repression occurring in the mesial temporal lobe may underlie the visuo-spatial impairment observed in patients with TDP-43 pathology. However, more research is needed to investigate how TDP-43 pathology affects the visuo-spatial abilities.

TDP-43 nuclear clearance: an early marker of TDP-43 loss of function and proteinopathy

TDP-43 pathology is characterized by TDP-43+ NCIs and nuclear clearance of TDP-43. Until now, few studies have focused on neurons with nuclear clearance of TDP-43 but without cytoplasmic inclusions [11, 12, 66, 81, 87]. An important function of TDP-43 is repressing the splicing of cryptic exons [13, 46, 50, 52, 57, 75]. Our previous study revealed that brains with nuclear clearance of TDP-43 without TDP-43+ NCIs had cryptic exon incorporation, indicating a loss of TDP-43 function when nuclear clearance is present in the absence of TDP-43 NCIs [81]. Others have confirmed that presence of TDP-43 regulated cryptic RNAs in AD brains [23]. In this study, we showed that 14.2% BLSA brains already had nuclear clearance of TDP-43 in the absence of TDP-43+ NCIs. Importantly, this phenomenon was first observed in individuals in their 50 s, about 10 years earlier than the earliest appearance of TDP-43+ NCIs. However, we did not find any nuclear clearance of TDP-43 in individuals younger than 50 years. We further used cryptic HDGFL2 antibody and RNA in situ hybridization to show that brains with nuclear clearance of TDP-43 exhibit cryptic exon inclusion and accumulation of cryptic peptide found in HDGFL2, an important pathogenic mechanism of TDP-43 proteinopathy. Recent studies have showed an association between TDP-43 pathology and increased tau pathology in the hippocampus, implying that TDP-43 pathology may exacerbate tau aggregation [58, 80, 85]. Our study demonstrated that not only brains with TDP-43+ NCIs but also brains with TDP-43 nuclear clearance without NCIs have higher burden of tau pathology in dentate gyrus of the hippocampus. This suggests that loss of TDP-43 splicing repression in neurons lacking NCI would initiate a pathogenic cascade that contributes to or accelerates tau aggregation. These findings indicate that the nuclear clearance of

TDP-43 is an early pathogenic event of TDP-43 proteinopathy, upstream to the TDP-43 NCIs, and that it precedes cognitive decline. Furthermore, our observations suggest that TDP-43 proteinopathy is more widespread in the population and appears at a younger age than currently believed. Further studies on the clinical and biological significance of neurons with nuclear clearance of TDP-43 but lacking TDP-43+ NCIs are necessary.

In summary, this study shows that loss of TDP-43 splicing repression is a seminal and early event in TDP-43 proteinopathy which is first manifested by neurons that exhibit nuclear clearance of TDP-43 lacking NCI as early as 50 s years of age, and then followed by TDP-43+ NCIs a decade later. Loss of TDP-43 splicing repression is associated with increased tau pathology, suggesting that such loss contributes or exacerbates the pathological conversion of tau in ADNC. LATE is common in brains with advanced ADNC, and has specific effects on the decline of memory and visuo-spatial ability in the aging population that are independent of AD.

Limitations

Our observations have some limitations. As all histological sections for immunohistochemistry and in situ hybridization were performed on tissues from the left hemisphere, therefore, possible asymmetries between the cerebral hemispheres cannot be detected. Another unavoidable limitation is the lack of cognitive evaluation of subjects in the young cohort. It is conceivable that the presence of TDP-43 abnormalities in the subjects from the young cohort could represent the early stage of FTLD. Some patients with FTLD exhibit anosognosia, which could not be ascertained without a cognitive evaluation.

Declarations

References

1. Amador-Ortiz C, Lin WL, Ahmed Z, Personett D, Davies P, Duara R et al (2007) TDP-43 immunoreactivity in hippocampal sclerosis and Alzheimer's disease. Ann Neurol 61:435–445. https://doi.org/10.1002/ana.21154

2. American Psychological Association (1987) Diagnostic and statistical manual of mental health disorders. American Psychiatric Association, Washington DC

3. Arnold SJ, Dugger BN, Beach TG (2013) TDP-43 deposition in prospectively followed, cognitively normal elderly individuals: correlation with argyrophilic grains but not other concomitant pathologies. Acta Neuropathol 126:51–57. https://doi.org/10.1007/s00401-013-1110-0

4. Bailly M, Destrieux C, Hommet C, Mondon K, Cottier JP, Beaufils E et al (2015) Precuneus and cingulate cortex atrophy and hypometabolism in patients with alzheimer's disease and mild cognitive impairment: MRI and (18)F-FDG PET quantitative analysis using FreeSurfer. Biomed Res Int 2015:583931. https://doi.org/10.1155/2015/583931

5. Bell WR, An Y, Kageyama Y, English C, Rudow GL, Pletnikova O et al (2019) Neuropathologic, genetic, and longitudinal cognitive profiles in primary age-related tauopathy (PART) and Alzheimer's disease. Alzheimers Dement 15:8–16. https://doi.org/10.1016/j.jalz.2018.07.215

6. Bennett DA, Wilson RS, Boyle PA, Buchman AS, Schneider JA (2012) Relation of neuropathology to cognition in persons without cognitive impairment. Ann Neurol 72:599–609. https://doi.org/10.1002/ana.23654

7. Benton AL (1968) Differential behavioral effects in frontal lobe disease. Neuropsychologia 6:53–60. https://doi.org/10.1016/0028-3932(68)90038-9

8. Boccia M, Sulpizio V, Nemmi F, Guariglia C, Galati G (2017) Direct and indirect parieto-medial temporal pathways for spatial navigation in humans: evidence from resting-state functional connectivity. Brain Struct Funct 222:1945–1957. https://doi.org/10.1007/s00429-016-1318-6

9. Boyle PA, Wang T, Yu L, Wilson RS, Dawe R, Arfanakis K et al (2021) To what degree is late life cognitive decline driven by

age-related neuropathologies? Brain 144:2166–2175. https://doi.org/10.1093/brain/awab092

10. Braak H, Braak E (1991) Neuropathological stageing of Alzheimer-related changes. Acta Neuropathol 82:239–259. https://doi.org/10.1007/bf00308809

11. Braak H, Del Tredici K (2018) Anterior cingulate cortex TDP-43 pathology in sporadic amyotrophic lateral sclerosis. J Neuropathol Exp Neurol 77:74–83. https://doi.org/10.1093/jnen/nlx104

12. Braak H, Ludolph AC, Neumann M, Ravits J, Del Tredici K (2017) Pathological TDP-43 changes in Betz cells differ from those in bulbar and spinal α-motoneurons in sporadic amyotrophic lateral sclerosis. Acta Neuropathol 133:79–90. https://doi.org/10.1007/s00401-016-1633-2

13. Brown AL, Wilkins OG, Keuss MJ, Hill SE, Zanovello M, Lee WC et al (2022) TDP-43 loss and ALS-risk SNPs drive mis-splicing and depletion of UNC13A. Nature 603:131–137. https://doi.org/10.1038/s41586-022-04436-3

14. Butler Pagnotti RM, Pudumjee SB, Cross CL, Miller JB (2023) Cognitive and clinical characteristics of patients with limbic-predominant age-related TDP-43 encephalopathy. Neurology 100:e2027–e2035. https://doi.org/10.1212/wnl.0000000000207159

15. Crary JF, Trojanowski JQ, Schneider JA, Abisambra JF, Abner EL, Alafuzoff I et al (2014) Primary age-related tauopathy (PART): a common pathology associated with human aging. Acta Neuropathol 128:755–766. https://doi.org/10.1007/s00401-014-1349-0

16. Cykowski MD, Arumanayagam AS, Powell SZ, Rivera AL, Abner EL, Roman GC et al (2022) Patterns of amygdala region pathology in LATE-NC: subtypes that differ with regard to TDP-43 histopathology, genetic risk factors, and comorbid pathologies. Acta Neuropathol 143:531–545. https://doi.org/10.1007/s00401-022-02416-5

17. Davidson YS, Raby S, Foulds PG, Robinson A, Thompson JC, Sikkink S et al (2011) TDP-43 pathological changes in early onset familial and sporadic Alzheimer's disease, late onset Alzheimer's disease and Down's syndrome: association with age, hippocampal sclerosis and clinical phenotype. Acta Neuropathol 122:703–713. https://doi.org/10.1007/s00401-011-0879-y

18. Delis DKJ, Kaplan E, Ober B (1987) California verbal learning test, research. The Psychological Corporation, New York

19. Dowling NM, Tomaszewski Farias S, Reed BR, Sonnen JA, Strauss ME, Schneider JA et al (2011) Neuropathological associates of multiple cognitive functions in two community-based cohorts of older adults. J Int Neuropsychol Soc 17:602–614. https://doi.org/10.1017/s1355617710001426

20. Driscoll I, Troncoso JC, Rudow G, Sojkova J, Pletnikova O, Zhou Y et al (2012) Correspondence between in vivo (11)C-PiB-PET amyloid imaging and postmortem, region-matched assessment of plaques. Acta Neuropathol 124:823–831. https://doi.org/10.1007/s00401-012-1025-1

21. Dugan AJ, Nelson PT, Katsumata Y, Shade LMP, Boehme KL, Teylan MA et al (2021) Analysis of genes (TMEM106B, GRN, ABCC9, KCNMB2, and APOE) implicated in risk for LATE-NC and hippocampal sclerosis provides pathogenetic insights: a retrospective genetic association study. Acta Neuropathol Commun 9:152. https://doi.org/10.1186/s40478-021-01250-2

22. Ekstrom RBH, Horace H (1976) Manual for kit of factor-referenced cognitive tests. Educational testing service, Princeton

23. Estades Ayuso V, Pickles S, Todd T, Yue M, Jansen-West K, Song Y et al (2023) TDP-43-regulated cryptic RNAs accumulate in Alzheimer's disease brains. Mol Neurodegener 18:57. https://doi.org/10.1186/s13024-023-00646-z

24. Filon JR, Intorcia AJ, Sue LI, Vazquez Arreola E, Wilson J, Davis KJ et al (2016) Gender differences in Alzheimer disease: brain atrophy, histopathology burden, and cognition. J Neuropathol Exp Neurol 75:748–754. https://doi.org/10.1093/jnen/nlw047

25. Flanagan ME, Cholerton B, Latimer CS, Hemmy LS, Edland SD, Montine KS et al (2018) TDP-43 neuropathologic associations in the Nun study and the Honolulu-Asia aging study. J Alzheimers Dis 66:1549–1558. https://doi.org/10.3233/jad-180162

26. Folstein MF, Folstein SE, McHugh PR (1975) "Mini-mental state". A practical method for grading the cognitive state of patients for the clinician. J Psychiatr Res 12:189–198. https://doi.org/10.1016/0022-3956(75)90026-6

27. Fuld P (1978) Psychological testing in the differential diagnosis of the dementias. Alzheimer's Dis Senile Demen Relat Disord 7:185–193

28. Hall A, Pekkala T, Polvikoski T, van Gils M, Kivipelto M, Lötjönen J et al (2019) Prediction models for dementia and neuropathology in the oldest old: the Vantaa 85+ cohort study. Alzheimers Res Ther 11:11. https://doi.org/10.1186/s13195-018-0450-3

29. Harrison WT, Lusk JB, Liu B, Ervin JF, Johnson KG, Green CL et al (2021) Limbic-predominant age-related TDP-43 encephalopathy neuropathological change (LATE-NC) is independently associated with dementia and strongly associated with arteriolosclerosis in the oldest-old. Acta Neuropathol 142:917–919. https://doi.org/10.1007/s00401-021-02360-w

30. Hawes Z, Sokolowski HM, Ononye CB, Ansari D (2019) Neural underpinnings of numerical and spatial cognition: an fMRI meta-analysis of brain regions associated with symbolic number, arithmetic, and mental rotation. Neurosci Biobehav Rev 103:316–336. https://doi.org/10.1016/j.neubiorev.2019.05.007

31. Hu WT, Josephs KA, Knopman DS, Boeve BF, Dickson DW, Petersen RC et al (2008) Temporal lobar predominance of TDP-43 neuronal cytoplasmic inclusions in Alzheimer disease. Acta Neuropathol 116:215–220. https://doi.org/10.1007/s00401-008-0400-4

32. Hu YT, Boonstra J, McGurran H, Stormmesand J, Sluiter A, Balesar R et al (2021) Sex differences in the neuropathological hallmarks of Alzheimer's disease: focus on cognitively intact elderly individuals. Neuropathol Appl Neurobiol 47:958–966. https://doi.org/10.1111/nan.12729

33. Hunter S, Hokkanen SRK, Keage HAD, Fleming J, Minett T, Polvikoski T et al (2020) TDP-43 related neuropathologies and phosphorylation state: associations with age and clinical dementia in the Cambridge City over-75s cohort. J Alzheimers Dis 75:337–350. https://doi.org/10.3233/jad-191093

34. Hyman BT, Phelps CH, Beach TG, Bigio EH, Cairns NJ, Carrillo MC et al (2012) National Institute on Aging-Alzheimer's Association guidelines for the neuropathologic assessment of Alzheimer's disease. Alzheimers Dement 8:1–13. https://doi.org/10.1016/j.jalz.2011.10.007

35. Irwin KE, Jasin P, Braunstein KE, Sinha I, Bowden KD, Moghekar A et al (2023) A fluid biomarker reveals loss of TDP-43 splicing repression in pre-symptomatic ALS. Nat Med (**in press**)

36. James BD, Wilson RS, Boyle PA, Trojanowski JQ, Bennett DA, Schneider JA (2016) TDP-43 stage, mixed pathologies, and clinical Alzheimer's-type dementia. Brain 139:2983–2993. https://doi.org/10.1093/brain/aww224

37. Jefferson-George KS, Wolk DA, Lee EB, McMillan CT (2017) Cognitive decline associated with pathological burden in primary age-related tauopathy. Alzheimers Dement 13:1048–1053. https://doi.org/10.1016/j.jalz.2017.01.028

38. Johnson DK, Storandt M, Morris JC, Galvin JE (2009) Longitudinal study of the transition from healthy aging to Alzheimer disease. Arch Neurol 66:1254–1259. https://doi.org/10.1001/archneurol.2009.158

39. Josephs KA (2018) Fitting TDP-43 into the APOE ε4 and neurodegeneration story. Lancet Neurol 17:735–737. https://doi.org/10.1016/s1474-4422(18)30288-6

40. Josephs KA, Murray ME, Tosakulwong N, Weigand SD, Serie AM, Perkerson RB et al (2019) Pathological, imaging and

genetic characteristics support the existence of distinct TDP-43 types in non-FTLD brains. Acta Neuropathol 137:227–238. https://doi.org/10.1007/s00401-018-1951-7

41. Josephs KA, Whitwell JL, Knopman DS, Hu WT, Stroh DA, Baker M et al (2008) Abnormal TDP-43 immunoreactivity in AD modifies clinicopathologic and radiologic phenotype. Neurology 70:1850–1857. https://doi.org/10.1212/01.wnl.0000304041.09418.b1

42. Josephs KA, Whitwell JL, Weigand SD, Murray ME, Tosakulwong N, Liesinger AM et al (2014) TDP-43 is a key player in the clinical features associated with Alzheimer's disease. Acta Neuropathol 127:811–824. https://doi.org/10.1007/s00401-014-1269-z

43. Kadokura A, Yamazaki T, Lemere CA, Takatama M, Okamoto K (2009) Regional distribution of TDP-43 inclusions in Alzheimer disease (AD) brains: their relation to AD common pathology. Neuropathology 29:566–573. https://doi.org/10.1111/j.1440-1789.2009.01017.x

44. Kapasi A, Yu L, Boyle PA, Barnes LL, Bennett DA, Schneider JA (2020) Limbic-predominant age-related TDP-43 encephalopathy, ADNC pathology, and cognitive decline in aging. Neurology 95:e1951–e1962. https://doi.org/10.1212/wnl.0000000000010454

45. Keage HA, Hunter S, Matthews FE, Ince PG, Hodges J, Hokkanen SR et al (2014) TDP-43 pathology in the population: prevalence and associations with dementia and age. J Alzheimers Dis 42:641–650. https://doi.org/10.3233/jad-132351

46. Klim JR, Williams LA, Limone F, Guerra San Juan I, Davis-Dusenbery BN, Mordes DA et al (2019) ALS-implicated protein TDP-43 sustains levels of STMN2, a mediator of motor neuron growth and repair. Nat Neurosci 22:167–179. https://doi.org/10.1038/s41593-018-0300-4

47. Kravitz DJ, Saleem KS, Baker CI, Mishkin M (2011) A new neural framework for visuospatial processing. Nat Rev Neurosci 12:217–230. https://doi.org/10.1038/nrn3008

48. Lin S (2020) Visuospatial memory alteration in Alzheimer's disease. Neurosci Bull 36:829–830. https://doi.org/10.1007/s12264-020-00560-0

49. Lin WL, Castanedes-Casey M, Dickson DW (2009) Transactivation response DNA-binding protein 43 microvasculopathy in frontotemporal degeneration and familial Lewy body disease. J Neuropathol Exp Neurol 68:1167–1176. https://doi.org/10.1097/NEN.0b013e3181baacec

50. Ling JP, Pletnikova O, Troncoso JC, Wong PC (2015) TDP-43 repression of nonconserved cryptic exons is compromised in ALS-FTD. Science 349:650–655. https://doi.org/10.1126/science.aab0983

51. Lopez OL, Kofler J, Chang Y, Berman SB, Becker JT, Sweet RA et al (2020) Hippocampal sclerosis, TDP-43, and the duration of the symptoms of dementia of AD patients. Ann Clin Transl Neurol 7:1546–1556. https://doi.org/10.1002/acn3.51135

52. Ma XR, Prudencio M, Koike Y, Vatsavayai SC, Kim G, Harbinski F et al (2022) TDP-43 represses cryptic exon inclusion in the FTD-ALS gene UNC13A. Nature 603:124–130. https://doi.org/10.1038/s41586-022-04424-7

53. Malek-Ahmadi M, Lu S, Chan Y, Perez SE, Chen K, Mufson EJ (2017) Cognitive domain dispersion association with Alzheimer's disease pathology. J Alzheimers Dis 58:575–583. https://doi.org/10.3233/jad-161233

54. McCarrey AC, An Y, Kitner-Triolo MH, Ferrucci L, Resnick SM (2016) Sex differences in cognitive trajectories in clinically normal older adults. Psychol Aging 31:166–175. https://doi.org/10.1037/pag0000070

55. McKeith IG, Dickson DW, Lowe J, Emre M, O'Brien JT, Feldman H et al (2005) Diagnosis and management of dementia with Lewy bodies: third report of the DLB Consortium. Neurology 65:1863–1872. https://doi.org/10.1212/01.wnl.0000187889.17253.b1

56. McKhann G, Drachman D, Folstein M, Katzman R, Price D, Stadlan EM (1984) Clinical diagnosis of Alzheimer's disease: report of the NINCDS-ADRDA Work Group under the auspices of Department of Health and Human Services Task Force on Alzheimer's Disease. Neurology 34:939–944. https://doi.org/10.1212/wnl.34.7.939

57. Melamed Z, López-Erauskin J, Baughn MW, Zhang O, Drenner K, Sun Y et al (2019) Premature polyadenylation-mediated loss of stathmin-2 is a hallmark of TDP-43-dependent neurodegeneration. Nat Neurosci 22:180–190. https://doi.org/10.1038/s41593-018-0293-z

58. Minogue G, Kawles A, Zouridakis A, Keszycki R, Macomber A, Lubbat V et al (2023) Distinct patterns of hippocampal pathology in Alzheimer's Disease with transactive response DNA-binding Protein 43. Ann Neurol. https://doi.org/10.1002/ana.26762

59. Mirra SS, Heyman A, McKeel D, Sumi SM, Crain BJ, Brownlee LM et al (1991) The Consortium to Establish a Registry for Alzheimer's Disease (CERAD). Part II. Standardization of the neuropathologic assessment of Alzheimer's disease. Neurology 41:479–486. https://doi.org/10.1212/wnl.41.4.479

60. Montine TJ, Corrada MM, Kawas C, Bukhari S, White L, Tian L et al (2022) Association of cognition and dementia with neuropathologic changes of Alzheimer disease and other conditions in the oldest-old. Neurology 99:e1067-1078. https://doi.org/10.1212/wnl.0000000000200832

61. Morris JC (1993) The clinical dementia rating (CDR): current version and scoring rules. Neurology 43:2412–2414. https://doi.org/10.1212/wnl.43.11.2412-a

62. Nag S, Barnes LL, Yu L, Wilson RS, Bennett DA, Schneider JA (2020) Limbic-predominant age-related TDP-43 encephalopathy in Black and White decedents. Neurology 95:e2056–e2064. https://doi.org/10.1212/wnl.0000000000010602

63. Nag S, Yu L, Boyle PA, Leurgans SE, Bennett DA, Schneider JA (2018) TDP-43 pathology in anterior temporal pole cortex in aging and Alzheimer's disease. Acta Neuropathol Commun 6:33. https://doi.org/10.1186/s40478-018-0531-3

64. Nag S, Yu L, Capuano AW, Wilson RS, Leurgans SE, Bennett DA et al (2015) Hippocampal sclerosis and TDP-43 pathology in aging and Alzheimer disease. Ann Neurol 77:942–952. https://doi.org/10.1002/ana.24388

65. Nag S, Yu L, Wilson RS, Chen EY, Bennett DA, Schneider JA (2017) TDP-43 pathology and memory impairment in elders without pathologic diagnoses of AD or FTLD. Neurology 88:653–660. https://doi.org/10.1212/wnl.0000000000003610

66. Nana AL, Sidhu M, Gaus SE, Hwang JL, Li L, Park Y et al (2019) Neurons selectively targeted in frontotemporal dementia reveal early stage TDP-43 pathobiology. Acta Neuropathol 137:27–46. https://doi.org/10.1007/s00401-018-1942-8

67. Nelson PT, Abner EL, Schmitt FA, Kryscio RJ, Jicha GA, Smith CD et al (2010) Modeling the association between 43 different clinical and pathological variables and the severity of cognitive impairment in a large autopsy cohort of elderly persons. Brain Pathol 20:66–79. https://doi.org/10.1111/j.1750-3639.2008.00244.x

68. Nelson PT, Brayne C, Flanagan ME, Abner EL, Agrawal S, Attems J et al (2022) Frequency of LATE neuropathologic change across the spectrum of Alzheimer's disease neuropathology: combined data from 13 community-based or population-based autopsy cohorts. Acta Neuropathol 144:27–44. https://doi.org/10.1007/s00401-022-02444-1

69. Nelson PT, Dickson DW, Trojanowski JQ, Jack CR, Boyle PA, Arfanakis K et al (2019) Limbic-predominant age-related TDP-43 encephalopathy (LATE): consensus working group report. Brain 142:1503–1527. https://doi.org/10.1093/brain/awz099

70. Nelson PT, Lee EB, Cykowski MD, Alafuzoff I, Arfanakis K, Attems J et al (2023) LATE-NC staging in routine neuropathologic

diagnosis: an update. Acta Neuropathol 145:159–173. https://doi.org/10.1007/s00401-022-02524-2

71. Neumann M, Sampathu DM, Kwong LK, Truax AC, Micsenyi MC, Chou TT et al (2006) Ubiquitinated TDP-43 in frontotemporal lobar degeneration and amyotrophic lateral sclerosis. Science 314:130–133. https://doi.org/10.1126/science.1134108

72. Newcombe F (1969) Missile wounds of the brain: a study of psychological deficits. Oxford University Press, Oxford

73. Parslow DM, Rose D, Brooks B, Fleminger S, Gray JA, Giampietro V et al (2004) Allocentric spatial memory activation of the hippocampal formation measured with fMRI. Neuropsychology 18:450–461. https://doi.org/10.1037/0894-4105.18.3.450

74. Petersen RC, Smith GE, Waring SC, Ivnik RJ, Tangalos EG, Kokmen E (1999) Mild cognitive impairment: clinical characterization and outcome. Arch Neurol 56:303–308. https://doi.org/10.1001/archneur.56.3.303

75. Prudencio M, Humphrey J, Pickles S, Brown AL, Hill SE, Kachergus JM et al (2020) Truncated stathmin-2 is a marker of TDP-43 pathology in frontotemporal dementia. J Clin Invest 130:6080–6092. https://doi.org/10.1172/jci139741

76. Reitan RM (1992) Trail making test: manual for administration and scoring. Reitan Neuropsychology Laboratory, Tucson

77. Robinson JL, Lee EB, Xie SX, Rennert L, Suh E, Bredenberg C et al (2018) Neurodegenerative disease concomitant proteinopathies are prevalent, age-related and APOE4-associated. Brain 141:2181–2193. https://doi.org/10.1093/brain/awy146

78. Robinson JL, Richardson H, Xie SX, Suh E, Van Deerlin VM, Alfaro B et al (2021) The development and convergence of co-pathologies in Alzheimer's disease. Brain 144:953–962. https://doi.org/10.1093/brain/awaa438

79. Smirnov DS, Salmon DP, Galasko D, Edland SD, Pizzo DP, Goodwill V et al (2022) TDP-43 pathology exacerbates cognitive decline in primary age-related tauopathy. Ann Neurol 92:425–438. https://doi.org/10.1002/ana.26438

80. Smith VD, Bachstetter AD, Ighodaro E, Roberts K, Abner EL, Fardo DW et al (2018) Overlapping but distinct TDP-43 and tau pathologic patterns in aged hippocampi. Brain Pathol 28:264–273. https://doi.org/10.1111/bpa.12505

81. Sun M, Bell W, LaClair KD, Ling JP, Han H, Kageyama Y et al (2017) Cryptic exon incorporation occurs in Alzheimer's brain lacking TDP-43 inclusion but exhibiting nuclear clearance of TDP-43. Acta Neuropathol 133:923–931. https://doi.org/10.1007/s00401-017-1701-2

82. Suthana NA, Ekstrom AD, Moshirvaziri S, Knowlton B, Bookheimer SY (2009) Human hippocampal CA1 involvement during allocentric encoding of spatial information. J Neurosci 29:10512–10519. https://doi.org/10.1523/jneurosci.0621-09.2009

83. Tan Q, Yalamanchili HK, Park J, De Maio A, Lu HC, Wan YW et al (2016) Extensive cryptic splicing upon loss of RBM17 and TDP43 in neurodegeneration models. Hum Mol Genet 25:5083–5093. https://doi.org/10.1093/hmg/ddw337

84. Thal DR, Rüb U, Orantes M, Braak H (2002) Phases of A beta-deposition in the human brain and its relevance for the development of AD. Neurology 58:1791–1800. https://doi.org/10.1212/wnl.58.12.1791

85. Tomé SO, Tsaka G, Ronisz A, Ospitalieri S, Gawor K, Gomes LA et al (2023) TDP-43 pathology is associated with increased tau burdens and seeding. Mol Neurodegener 18:71. https://doi.org/10.1186/s13024-023-00653-0

86. Uchino A, Takao M, Hatsuta H, Sumikura H, Nakano Y, Nogami A et al (2015) Incidence and extent of TDP-43 accumulation in aging human brain. Acta Neuropathol Commun 3:35. https://doi.org/10.1186/s40478-015-0215-1

87. Vatsavayai SC, Yoon SJ, Gardner RC, Gendron TF, Vargas JN, Trujillo A et al (2016) Timing and significance of pathological features in C9orf72 expansion-associated frontotemporal dementia. Brain 139:3202–3216. https://doi.org/10.1093/brain/aww250

88. Wang SJ, Guo Y, Ervin JF, Lusk JB, Luo S (2022) Neuropathological associations of limbic-predominant age-related TDP-43 encephalopathy neuropathological change (LATE-NC) differ between the oldest-old and younger-old. Acta Neuropathol 144:45–57. https://doi.org/10.1007/s00401-022-02432-5

89. Williams OA, An Y, Armstrong NM, Kitner-Triolo M, Ferrucci L, Resnick SM (2020) Profiles of cognitive change in preclinical and prodromal alzheimer's disease using change-point analysis. J Alzheimers Dis 75:1169–1180. https://doi.org/10.3233/jad-191268

90. Williams OA, An Y, Armstrong NM, Shafer AT, Helphrey J, Kitner-Triolo M et al (2019) Apolipoprotein E ε4 allele effects on longitudinal cognitive trajectories are sex and age dependent. Alzheimers Dement 15:1558–1567. https://doi.org/10.1016/j.jalz.2019.07.011

91. Wilson JR, De Fries JC, McClearn GE, Vanderberg SG, Johnson RC, Rashad MN (1975) Cognitive abilities: use of family data as a control to assess sex and age differences in two ethnic groups. Int J Aging Hum Dev 6:261–276. https://doi.org/10.2190/bbjp-xkug-c6ew-kyb7

92. Wilson RS, Yu L, Trojanowski JQ, Chen EY, Boyle PA, Bennett DA et al (2013) TDP-43 pathology, cognitive decline, and dementia in old age. JAMA Neurol 70:1418–1424. https://doi.org/10.1001/jamaneurol.2013.3961

93. Xu Y (2018) The posterior parietal cortex in adaptive visual processing. Trends Neurosci 41:806–822. https://doi.org/10.1016/j.tins.2018.07.012

94. Yang HS, Yu L, White CC, Chibnik LB, Chhatwal JP, Sperling RA et al (2018) Evaluation of TDP-43 proteinopathy and hippocampal sclerosis in relation to APOE ε4 haplotype status: a community-based cohort study. Lancet Neurol 17:773–781. https://doi.org/10.1016/s1474-4422(18)30251-5

95. Zhu L, Wang Z, Du Z, Qi X, Shu H, Liu D et al (2020) Impaired parahippocampal gyrus-orbitofrontal cortex circuit associated with visuospatial memory deficit as a potential biomarker and interventional approach for Alzheimer disease. Neurosci Bull 36:831–844. https://doi.org/10.1007/s12264-020-00498-3